HHS Public Access

Author manuscript

Nat Med. Author manuscript; available in PMC 2021 June 04.

Published in final edited form as:

Nat Med. 2020 August ; 26(8): 1285–1294. doi:10.1038/s41591-020-0985-2.

Assessment of cognitive and neural recovery in survivors of pediatric brain tumors in a pilot clinical trial using metformin

Ramy Ayoub[1,2,15], **Rebecca M. Ruddy**[3,15], **Elizabeth Cox**[1,2], **Adeoye Oyefiade**[1,2], **Daniel Derkach**[3], **Suzanne Laughlin**[4,5], **Benjamin Ades-aron**[6], **Zahra Shirzadi**[7,8], **Els Fieremans**[6], **Bradley J. Macintosh**[7,8], **Cynthia B. de Medeiros**[1], **Jovanka Skocic**[1], **Eric Bouffet**[9,10], **Freda D. Miller**[1,3,11,12], **Cindi M. Morshead**[3,13,14], **Donald J. Mabbott**[1,2]

[1]Neurosciences and Mental Health Program, Research Institute, Hospital for Sick Children, Toronto, Ontario, Canada.

[2]Department of Psychology, University of Toronto, Toronto, Ontario, Canada.

[3]Institute of Medical Science, University of Toronto, Toronto, Ontario, Canada.

[4]Diagnostic Imaging, Hospital for Sick Children, Toronto, Ontario, Canada.

[5]Department of Medical Imaging, University of Toronto, Toronto, Ontario, Canada.

[6]Center for Biomedical Imaging, Department of Radiology, New York University Grossman School of Medicine, New York, NY, USA.

[7]Department of Medical Biophysics, University of Toronto, Toronto, Ontario, Canada.

Correspondence and requests for materials should be addressed to C.M.M. or D.J.M. cindi.morshead@utoronto.ca; donald.mabbott@sickkids.ca.

Author contributions

Conceptualization, R.M.R., E.B., F.D.M., C.M.M. and D.J.M.; methodology, R.A., R.M.R., E.B., C.M.M. and D.J.M.; software, B.A., Z.S., E.F. and B.J.M.; formal analysis, R.A., R.M.R., E.C., A.O., D.D., C.B.d.M., E.B., C.M.M. and D.J.M.; investigation, R.M.R.,C.B.d.M., J.S., E.B., C.M.M. and D.J.M.; resources, S.L., B.A., Z.S., E.F., B.J.M., E.B.,C.M.M. and D.J.M.; data curation, R.A., R.M.R., D.D., C.B.d.M. and J.S.; writing–original draft, R.A., R.M.R., F.D.M., C.M.M. and D.J.M.; writing–review and editing, R.A., R.M.R., E.C., A.O., D.D., B.A., Z.S., E.F., B.J.M., C.B.d.M., J.S., E.B., F.D.M., C.M.M. and D.J.M.; supervision, C.M.M. and D.J.M.; project administration, C.B.d.M., J.S. and D.J.M.; funding acquisition, F.D.M., C.M.M. and D.J.M.

Competing interests

E.F. is a co-inventor and the New York University Grossman School of Medicine is owner of the denoising technology used in this manuscript as part of the routine data image processing pipeline; a patent application has been filed and is pending. E.F., B.A. and the New York University Grossman School of Medicine are shareholders and have advisory roles at Microstructure Imaging, Inc. The remaining authors do not have any competing interests to declare.

Extended data is available for this paper at https://doi.org/10.1038/s41591-020-0985-2.

Supplementary information is available for this paper at https://doi.org/10.1038/s41591-020-0985-2.

Peer review information Kate Gao and Javier Carmona were the primary editors on this article and managed its editorial process and peer review in collaboration with the rest of the editorial team.

Reporting Summary. Further information on research design is available in the Nature Research Reporting Summary linked to this article.

Publisher's note Springer Nature remains neutral with regard to jurisdictional claims in published maps and institutional affiliations.

Online content

Any methods, additional references, Nature Research reporting summaries, source data, extended data, supplementary information, acknowledgements, peer review information; details of author contributions and competing interests; and statements of data and code availability are available at https://doi.org/10.1038/s41591-020-0985-2.

[8]Hurvitz Brain Sciences, Sunnybrook Research Institute, University of Toronto, Toronto, Ontario, Canada.

[9]Division of Haematology/Oncology, Hospital for Sick Children, Toronto, Ontario, Canada.

[10]Department of Paediatrics, University of Toronto, Toronto, Ontario, Canada.

[11]Department of Molecular Genetics, University of Toronto, Toronto, Ontario, Canada.

[12]Department of Physiology, University of Toronto, Toronto, Ontario, Canada.

[13]Institute of Biomaterials and Biomedical Engineering, University of Toronto, Toronto, Ontario, Canada.

[14]Division of Anatomy, Department of Surgery, University of Toronto, Toronto, Ontario, Canada.

[15]These authors contributed equally: Ramy Ayoub, Rebecca M. Ruddy.

Abstract

We asked whether pharmacological stimulation of endogenous neural precursor cells (NPCs) may promote cognitive recovery and brain repair, focusing on the drug metformin, in parallel rodent and human studies of radiation injury. In the rodent cranial radiation model, we found that metformin enhanced the recovery of NPCs in the dentate gyrus, with sex-dependent effects on neurogenesis and cognition. A pilot double-blind, placebo-controlled crossover trial was conducted (ClinicalTrials.gov, NCT02040376) in survivors of pediatric brain tumors who had been treated with cranial radiation. Safety, feasibility, cognitive tests and MRI measures of white matter and the hippocampus were evaluated as endpoints. Twenty-four participants consented and were randomly assigned to complete 12-week cycles of metformin (A) and placebo (B) in either an AB or BA sequence with a 10-week washout period at crossover. Blood draws were conducted to monitor safety. Feasibility was assessed as recruitment rate, medication adherence and procedural adherence. Linear mixed modeling was used to examine cognitive and MRI outcomes as a function of cycle, sequence and treatment. We found no clinically relevant safety concerns and no serious adverse events associated with metformin. Sequence effects were observed for all cognitive outcomes in our linear mixed models. For the subset of participants with complete data in cycle 1, metformin was associated with better performance than placebo on tests of declarative and working memory. We present evidence that a clinical trial examining the effects of metformin on cognition and brain structure is feasible in long-term survivors of pediatric brain tumors and that metformin is safe to use and tolerable in this population. This pilot trial was not intended to test the efficacy of metformin for cognitive recovery and brain growth, but the preliminary results are encouraging and warrant further investigation in a large multicenter phase 3 trial.

The mammalian brain contains resident precursor cell populations that contribute to neural development and persist into adulthood. These findings have led to the idea that activation of endogenous precursors may promote tissue repair[1]. This is particularly intriguing with regard to the human brain, which displays limited self-repair but contains distinct populations of NPCs. These include the multipotent subventricular zone (SVZ) and hippocampal NPCs that generate neurons and glia, as well as the more biased oligodendrocyte precursor cells (OPCs) that generate oligodendrocytes throughout life[2]. In

rodents, NPCs in the forebrain SVZ contribute to olfactory memory, while NPCs in the hippocampal dentate gyrus (DG) contribute to spatial learning and memory, suggesting important functional roles for postnatal neurogenesis[3,4]. Agents have been identified that can induce proliferation and differentiation of NPCs in vivo and promote rodent brain repair[5,6]; however, it is unknown whether this brain repair strategy is viable in humans.

Metformin is a well-established oral hypoglycemic agent that is used to safely treat adults and children with diabetes, metabolic disorders and obesity[7-11]. Studies in adult mice showed that systemic administration of metformin resulted in increased neurogenesis by activating the atypical protein kinase C (aPKC)–CREB-binding protein (CBP) pathway in NPCs[4,12]. Importantly, metformin also improved spatial memory, which requires hippocampal neurogenesis[4]. Systemic metformin was also used in a murine model of neonatal brain injury, where it promoted recovery of sensory-motor and cognitive function concomitantly with NPC activation, neurogenesis and oligodendrogenesis[13,14]. Metformin was also shown to ameliorate a disease-dependent decrease in hippocampal neurogenesis and spatial memory formation, independently of its effects on hyperglycemia[15]. These preclinical data, together with studies showing that metformin enhances the survival and differentiation of human NPCs[4,16], raise the exciting possibility that metformin may recruit endogenous NPCs to promote human neural repair and cognitive recovery.

Survivors of pediatric brain tumors who were treated with cranial radiation are an ideal population in which to study the potential benefits of metformin for brain injury. First, white matter and the hippocampus, both known niches for human NPCs, are the structures most damaged by cranial radiation[17-20]. Second, these children experience cognitive impairment related to white matter damage and hippocampal atrophy[21-24]. These observations are paralleled in rodent models of cranial radiation, in which deficits in olfaction and spatial memory are coupled with reduced neurogenesis, depletion of OPCs and impaired myelination[17,25-28]. Finally, while adult human neurogenesis is debated[29,30], there is a general consensus that NPCs are present and active in the hippocampus, forebrain and white matter niches in children and adolescents[31,32].

To examine the therapeutic potential of metformin in cognition and brain repair, we conducted parallel rodent and human studies of radiation injury using analogous behavioral assays. First, we tested the cellular and behavioral outcomes in a preclinical mouse model of brain injury acquired from cranial radiation. Administration of cranial radiation to juvenile mice led to an acute radiation-induced depletion of NPCs in both the SVZ and DG. Spontaneous recovery of the stem cell pool was seen in the SVZ, but not in the DG. However, metformin administration was sufficient to recover DG NPCs. Cognitive deficits resulting from cranial radiation were rescued with metformin treatment in females, but not males, coinciding with the rescue of neurogenesis.

We also conducted a pilot clinical trial (ClinicalTrials.gov, NCT02040376) to examine the safety and feasibility of metformin administration in survivors of pediatric brain tumors who had completed primary treatment, including cranial radiation, from 2 to 15 years previously (Fig. 1). We found that metformin was safe to use in these patients with high medication and procedural adherence. When we explored specific memory measures, we observed that these

outcomes may be sensitive for evaluating metformin-mediated recovery. Taken together, our findings support further investigation of metformin as a new therapeutic treatment for a previously untreatable brain injury in a phase 3 trial.

Results

Radiation-induced reduction in the neural stem cell pool is rescued by metformin.

To test whether metformin acts on stem and progenitor cells following cranial radiation to the young brain, we explored its effects in both the SVZ lining the lateral ventricles and the DG of the hippocampus in a preclinical mouse model[28]. Juvenile mice (postnatal day (P) 17) received 8 Gy cranial radiation, and the effects on the neural stem cell pool were assessed at early (1–2 d after radiation) and late (5 weeks after radiation) time points using an in vitro neurosphere assay (Fig. 2a). In this assay, the number of neurospheres reflects the number of stem cells. We observed significant reductions in neurosphere number from the SVZ (53% reduction; $t_{(14)} = 2.81$, $P = 0.01$; Fig. 2b) and DG (75% reduction; $t_{(5)} = 4.04$, $P = 0.01$; Fig. 2c) at early times (1–2 d) after radiation. The stem cell population in the SVZ recovered to control levels at 5 weeks after radiation (control mice versus mice receiving radiation, $P = 0.99$; Fig. 2d); however, the deficit in the DG stem cell pool persisted (44% reduction; control mice versus mice receiving radiation, $P = 0.002$; Fig. 2e). Strikingly, mice that received 25 d of metformin (200 mg per kg daily) starting 1 d after radiation showed complete recovery in the DG (control mice versus mice receiving radiation + metformin, $P = 0.99$; Fig. 2e). Metformin-treated controls (non-radiated mice) showed no change in neurosphere numbers (SVZ: $t_{(38)} = 0.10$, $P = 0.92$; DG: $t_{(20)} = 0.90$, $P = 0.38$; Extended Data Fig. 1a,b). Notably, the metformin-mediated recovery in DG neurospheres was not sex dependent (control mice versus mice receiving radiation + metformin: females, $P = 0.92$; males, $P = 0.93$; Extended Data Fig. 2a-d). Hence, metformin treatment for 25 d starting 1 d after radiation was sufficient to enhance recovery of the DG stem cell pool.

We next examined the effects of radiation and metformin on stem cell progeny. In the SVZ, the number of neuroblasts (positive for doublecortin (DCX^+)) returned to control levels by 5 weeks after radiation, with or without metformin treatment, in both females ($F_{(2,9)} = 2.453$, $P = 0.14$) and males ($F_{(2,14)} = 1.77$, $P = 0.21$; Fig. 2f-i). Conversely, in the DG, there was a significant reduction in the number of DCX^+ neuroblasts and metformin treatment rescued this deficit in females (control mice versus mice receiving radiation, $P = 0.01$; control mice versus mice receiving radiation + metformin, $P = 0.30$; Fig. 2j,k) but not males (control mice versus mice receiving radiation, $P = 0.008$; control mice versus mice receiving radiation + metformin, $P = 0.03$; Fig. 2l,m). Together, these findings show regionally distinct recovery of SVZ and DG NPCs following radiation and sex-dependent effects of metformin on the NPC pools.

Metformin treatment improves cognitive outcomes in mice.

We next asked whether metformin administration was sufficient to rescue functional impairments resulting from cranial radiation. Cognitive performance was assessed after cranial radiation and metformin treatment (Fig. 2a). We found that females, but not males, showed a significant deficit in the Y maze task (control mice versus mice receiving

radiation: females, $P = 0.02$; males, $P = 0.89$), which assesses working memory, and this impairment was completely rescued with metformin treatment (control mice versus mice receiving radiation + metformin: females, $P = 0.71$; Fig. 2n-p). Radiated males, but not females, displayed a significant deficit in spatial memory in the novel place recognition task (control mice versus mice receiving radiation: females, $P = 0.55$; males, $P = 0.02$), which was not rescued by metformin treatment (control mice versus mice receiving radiation + metformin: males, $P = 0.02$; Fig. 2q-s). No significant effects were seen in non-radiated, metformin-treated mice in the Y maze task ($t_{(67)} = 0.34$, $P = 0.74$) or the novel place recognition task ($t_{(59)} = 0.70$, $P = 0.48$; Extended Data Fig. 1c,d). No impairments in locomotor activity or anxiety, as measured using the open-field maze (females: $F_{(2,42)} = 0.62$, $P = 0.54$; males: $F_{(2,52)} = 0.40$, $P = 0.67$) and elevated plus maze (females: $F_{(2,13)} = 1.26$, $P = 0.32$; males: $F_{(2,13)} = 0.78$, $P = 0.48$), respectively, were observed (Extended Data Fig. 3a-e). These results demonstrate that radiation leads to differential cognitive deficits in females and males and that metformin can rescue cognitive impairments in female mice[14].

Pilot clinical trial.

We conducted a pilot randomized, double-blind, placebo-controlled trial with crossover in survivors of pediatric brain tumors with primary endpoints of safety and feasibility and secondary endpoints of cognitive and magnetic resonance imaging (MRI) measures. Twenty-four participants were enrolled (recruitment rate of 21%; see Extended Data Fig. 4 for a consort diagram) and randomly assigned to complete 12-week cycles of metformin (A) and placebo (B) in either an AB or BA sequence. At the point of crossover, there was a 10-week washout period in which neither group received any treatment. During the first week of each treatment cycle, a daily dose of 500 mg m^{-2} of metformin or placebo was administered orally (p.o.); the dose was increased to 1,000 mg m^{-2} daily beginning in the second week and continuing for the remainder of the 12-week cycle. A prespecified sample of 30 and expected recruitment rate of 25% were not reached, and the trial was discontinued as no further eligible participants consented (Methods).

Participant characteristics are presented in Table 1. Patients were treated with either focal or cranial-spinal radiation for a brain tumor. The two sequence groups did not differ in terms of sex, age at baseline assessment, age at time of diagnosis, radiation treatment and number of years after treatment. However, at baseline, participants treated with metformin first (AB sequence group) included a greater proportion of participants with cranial nerve deficits ($\chi^2_{(1)} = 5.04$, $P = 0.03$), cerebellar signs (that is, ataxia, dysmetria and dysdiadochokinesia) ($\chi^2_{(1)} = 6.17$, $P = 0.01$), mutism after surgery deficits ($\chi^2_{(1)} = 5.04$, $P = 0.03$) and treatment with a tumor bed versus posterior fossa radiation boost ($\chi^2_{(1)} = 6.40$, $P = 0.04$) than those treated with placebo first (BA sequence group).

Safety and adherence.

Blood draws were conducted and complete blood cell counts, blood differentials, platelet counts, liver function tests, and measures of serum creatinine and lactate levels were obtained at all study visits. No clinically relevant changes were observed for any participant during metformin treatment across tests. The most frequent adverse events (grade range from 1–3) included vomiting, diarrhea, headache, fatigue and nausea (Fig. 3a). No serious

adverse events such as lactic acidosis occurred. Metformin treatment was associated with an average of 2.5 adverse events and placebo with an average of 1.6 adverse events across participants. A greater number of gastrointestinal disorders were evident during metformin versus placebo treatment, corresponding to 24 versus 8 minor adverse events, respectively. Adherence to study treatment and procedures was high (Fig. 3b).

Assessment of cognitive function.

Raw scores for tests of working memory (List Sorting Working Memory (LSWM) and Picture Sequence Memory Test (PSM) from the National Institutes of Health (NIH) Toolbox[33]); declarative memory (Children's Auditory Verbal Learning Test-2 (CAVLT-2)[34]/Rey Auditory Verbal Learning Test (RAVLT)[35]); and information processing speed (average reaction time across select tests from the Cambridge Neuropsychological Test Automated Battery (CANTAB)[36]) were dependent variables: these cognitive functions are compromised in survivors of pediatric brain tumors. Separate general linear mixed models were used for each cognitive test with two sets of outcomes (outcomes 1 and 2 corresponding to the test results at the end of the first and second 12-week treatment cycles, respectively). As independent variables, we examined the fixed effects of cycle (first versus second 12-week treatment cycle), treatment (metformin versus placebo) and sequence (metformin first, placebo second (AB) versus placebo first, metformin second (BA)) on test scores from each measure (that is, item accuracy and/or latency). Baseline test scores (from baseline 1 and 2 corresponding to the start of the first and second 12-week treatment cycles, respectively), each of which corresponded to one outcome test score, were included as a fixed covariate. A random effect for participant as an independent variable accounted for the correlation between the two independent baseline and outcome test scores for each participant. In a series of separate models, we further assessed fixed effects while adjusting separately for the presence of cranial nerve deficits, posterior fossa mutism, cerebellar neurological signs and dose and field of radiation. All models were corrected for multiple comparisons (false discovery rate (FDR) $q < 0.10$).

Greater total numbers of correct responses on LSWM ($F_{(1,8)} = 5.07$, $P = 0.05$; Fig. 4a,b and Extended Data Fig. 5a) and decreased average latency on the CANTAB tests ($F_{(1,9)} = 5.67$, $P = 0.04$; Fig. 4c,d and Extended Data Fig. 5b) were observed for treatment with metformin versus placebo. These treatment effects did not survive multiple-comparisons correction. There were sequence effects that survived multiple-comparisons correction (Extended Data Fig. 5a-c) for (1) LSWM ($F_{(1,24)} = 6.46$, $P = 0.02$, $q = 0.09$), (2) average latency across the CANTAB tests ($F_{(1,18)} = 7.06$, $P = 0.03$, $q = 0.09$) and (3) immediate recall on the CAVLT-2/RAVLT ($F_{(1,23)} = 7.37$, $P = 0.01$, $q = 0.09$). Better performance was observed for the AB versus BA sequence group on all cognitive tests at outcome assessment (Fig. 4a-f and Extended Data Fig. 5a-c). The significant effects were not affected by inclusion of medical and demographic variables considered in the models. No effects of cycle were observed. Finally, no effects were observed for level of learning, interference and delayed recall on the CAVLT-2/RAVLT or the PSM (all $P > 0.10$).

When a sequence effect is observed in a crossover design, data from the first cycle only should be used to examine treatment effects[37]. Hence, we used a post hoc Mann–Whitney U

(MW) test (because of the small sample size) to compare median test scores between the metformin and placebo conditions at cycle 1 outcome following the identification of a significant sequence effect. Significant metformin treatment effects were observed at cycle 1 outcome for LSWM (metformin median = 2; placebo median = −3; MW = 2.10, $P = 0.02$, $q = 0.04$; metformin $n = 3$, placebo $n = 5$) and auditory-verbal memory (metformin median = 1; placebo median = −1; MW = 2.10, $P = 0.02$, $q = 0.04$; metformin $n = 3$, placebo $n = 5$). The treatment effect of metformin for average reaction time on the CANTAB tests approached significance (metformin median = −178.74 ms; placebo median = 113.98 ms; MW = 1.58, $P = 0.06$, $q = 0.07$; metformin $n = 4$, placebo $n = 4$). Notably, all effects were in the direction reflecting positive impact of metformin.

Assessment of corpus callosum white matter.

To ask whether metformin might promote white matter repair in humans as reported in previous studies of the young brain in injured rodents, we performed diffusion kurtosis imaging (DKI) (Fig. 1d). White matter tract integrity model (WMTI)[38] metrics sensitive to myelin were calculated, specifically, the axonal water fraction (AWF) and extra-axonal radial diffusivity ($D_{e,\perp}$)[39]. We focused on the corpus callosum because it is immediately adjacent to SVZ NPCs and contains OPCs, both of which can contribute to oligodendrogenesis (Fig. 5a-e). Linear mixed modeling as described above was conducted.

A significant increase in AWF within the corpus callosum (Fig. 5f,g) was observed as a function of metformin treatment ($F_{(U)} = 11.03$, $P = 0.04$, $q = 0.08$). A significant sequence effect was also present ($F_{(1,17)} = 7.65$, $P = 0.01$, $q = 0.04$; Extended Data Fig. 5d): AWF was greater for the AB group than for the BA group. These effects were not affected by inclusion of medical and demographic variables considered in the models. We found no significant differences in $D_{e,\perp}$ (all $P > 0.05$).

When we conducted exploratory analyses of differences in AWF within only cycle 1 using the MW test, the effects of metformin were not significant (metformin median = 0.004; placebo median = −0.012; MW = 1.50, $P < 0.07$; metformin $n = 4$, placebo $n = 2$).

We also conducted voxel-wise analyses of AWF and $D_{e,\perp}$ using tract-based spatial statistics (TBSS)[40] to examine whole-brain white matter. No differences were observed from before to after metformin treatment (Extended Data Fig. 6), and we therefore did not carry out further linear mixed modeling of cycle, treatment or sequence.

Assessment of hippocampal blood flow.

Metformin may enhance genesis of new neurons in both the forebrain and hippocampal DG, as we observed in our preclinical work. We therefore measured cerebral blood flow (CBF) within the hippocampus of participants (Extended Data Fig. 7a-c), because cell proliferation and angiogenesis are correlated and increased hippocampal blood flow may thus reflect neurogenesis[41]. We obtained an estimate of CBF within the left and right hippocampi (Fig. 1d and Extended Data Fig. 7d-g). No significant differences in CBF in either the left or right hippocampus were observed as a function of metformin treatment, cycle or sequence (all $P > 0.05$).

Discussion

Our rodent studies and human pilot trial support the potential of metformin-mediated promotion of cognitive and neural recovery following radiation injury. First, in juvenile mice, cranial radiation induces an acute depletion of NPCs in both the SVZ and DG and there is differential recovery between these regions, in line with similar models of cranial radiation[27]. Interestingly, in this preclinical model, metformin treatment was sufficient to rescue neurogenesis in the DG in a sex-dependent manner, with females, but not males, responsive to metformin treatment. The enhanced neurogenesis was correlated with improved performance on a working memory task in females but not males. Second, for our primary endpoint in the pilot trial, we found that metformin is safe to use and tolerable in survivors of pediatric brain tumors. While an increased number of mild gastrointestinal adverse events were evident, consistent with the known effects of metformin, these were tolerable and no serious adverse events were observed. Secondarily, we provide evidence that measures of memory may be useful for exploring efficacy in future phase 3 trials in this population. Our preliminary evidence is particularly encouraging in light of the typical trajectory observed in survivors of pediatric brain tumors treated with radiation, including poorer memory, slower information processing speed and greater compromise of white matter over time[21-24].

Because this was a pilot trial with a small sample size, it will be critical to evaluate metformin in larger efficacy trials with prespecified primary and secondary outcomes and more efficient trial design. Our work provides valuable information for designing such a trial and delineating relevant outcomes. Our preclinical studies support examining the impact of sex in future trials[14]. The sex-dependent effects of radiation and metformin on rescuing neuroblasts and cognitive function we observed in mice suggest that females may in particular benefit from metformin. This is notable as human studies suggest that females treated for brain tumors are particularly vulnerable to cognitive effects late in childhood[24]. Furthermore, the consistent effects of metformin on memory in both rodents and children/adolescents highlight this domain as an important outcome.

Our previous work has demonstrated that the sex-dependent effects on NPCs can be accounted for by differences in the microenvironment[14]. Furthermore, our findings are consistent with cranial radiation differentially affecting NPCs and cognition in males and females[20]. As such, perturbing the microenvironment through radiation may differentially affect the male and female niches, leading to sex-dependent effects of metformin. While further investigation of the mechanisms of action by metformin are warranted, the preclinical data herein demonstrate that metformin treatment enhances both cellular and functional recovery following juvenile cranial radiation.

We used a crossover design (1) to ensure that all participants had access to metformin, considering the potential positive effects on brain health—there are very few interventions that offer the possibility of improved outcomes for these vulnerable patients; (2) to maximize in a pilot trial the opportunity to use the data acquired, as in this design a participant serves as their own control; and (3) because the resulting injury following pediatric brain tumor treatment is relatively stable and a crossover design is appropriate for

such injury. However, the presence of sequence effects confounded potential treatment effects. A greater frequency of patients in the AB group experienced more severe acute injury at the time of diagnosis owing to the effects of the tumor and surgery (that is, cranial nerve deficits, cerebellar signs and posterior fossa mutism) in comparison to the BA group, but a smaller proportion of these participants were treated with more intensive radiation (that is, with a boost of radiation to the tumor bed as opposed to the entire posterior fossa). Notably, greater severity of acute injury is associated with poor cognitive outcomes, irrespective of the intensity of radiation therapy[42,43]. Perhaps metformin has effects in the context of greater acute injury, irrespective of radiation treatment intensity: with greater acute injury, the AB group may have had more potential for metformin-mediated recovery than the BA group. Future animal work is needed to examine the effects of metformin as a function of injury severity.

Although we used the recommended procedure of examining outcomes only from the first cycle in the presence of sequence effects, we note that this approach has been associated with over-inflation of significance values and caution is warranted[44]. As our goal was to identify outcomes potentially sensitive to the effects of metformin to be carried forward for further testing in an efficacy trial, we think that using this approach was warranted in our pilot trial. In a future phase 3 trial, it will be critical to use a more efficient design not susceptible to sequence effects, such as a parallel arm trial, and to stratify arms by presence of residual symptoms following surgery and radiation protocols. Furthermore, to increase recruitment rates in future, trial strategies to decrease logistical challenges limiting participation should be considered, including decreasing the number of study visits through online, virtual or telephone monitoring, conducting trial visits during evenings and weekends, and providing greater support for travel arrangements.

Our trial was limited by an uneven distribution of medical and demographic factors between the sequence groups, missing data, a wide range in age and time since diagnosis, and a small number of patients, and its results must be interpreted with caution. Despite these limitations, our memory findings are consistent with previous animal studies and our preclinical rodent studies. In mice, metformin administration increases hippocampal neurogenesis and enhances learning and memory[4]. Intriguingly, we observed a metformin-related increase in auditory-verbal recall and working memory in a small number of participants following cycle 1. In humans, audio-verbal memory has been associated with hippocampal subfields involved in neurogenesis, including the DG[45,46]. Although working memory is mediated primarily by prefrontal regions, it has also been associated with the hippocampus because of encoding requirements[47]. Post hoc analyses of a previous metformin trial for weight control in children with autism did not show any benefits to visual-spatial memory performance[11]. In line with this, we also did not observe significant improvements in visual-spatial memory. Furthermore, we did not observe differences in hippocampal CBF associated with metformin treatment. Finally, our findings of increased AWF within the corpus callosum following treatment are intriguing but, when considering that there were sequence effects, a very small sample size and that post hoc analyses of cycle 1 were not significant, must be considered very preliminary: we think there is value in drawing attention to white matter as an outcome to be evaluated in a future phase 3 trial.

While some clinical trials have evaluated stem cell transplantation within the central nervous system[48,49], we present new evidence that repair of endogenous stem cells may be viable. Our findings support metformin as safe and feasible to use in survivors of pediatric brain tumors. There is evidence that metformin promotes repair and behavioral recovery by mechanisms other than activation of NPCs, including by reducing chronic inflammation in a rodent model of Alzheimer's disease[50] and regulating signaling pathways of proteins important for synaptogenesis in a rodent model of fragile X syndrome[51]. In older adults with diabetes and other disorders, metformin is associated with decreased rates of dementia and improved cognition, particularly in audio-verbal memory[52,53]. Metformin has shown promise for improving behavior and language in children with a neurodevelopmental disorder[54]. Given the considerable preclinical support and therapeutic role metformin may have for other disorders[51,54], this medication has substantial potential for ameliorating the impact of early brain insult. Furthermore, the possibility of multimodal therapy, combining metformin with strategies that foster activity-dependent myelination, is intriguing[55]. Larger clinical trials are needed to determine efficacy, identify optimal dosing and timing for initiation of treatment, test treatment duration effects and test the impact of sex. Although our work does not establish the efficacy of metformin for cognitive recovery and brain growth following acquired brain injury, the combined findings from our rodent studies and human trial are encouraging and justify a future phase 3 trial.

Methods

Rodent studies.

Animals.—All experiments were performed in accordance with institutional guidelines approved by the Animal Care Committee at the University of Toronto (Animal Use Protocol 20011476). C57BL/6 mice were purchased from Charles River Laboratories or bred in house. Following weaning, mice were group housed (maximum of four mice per cage) in a 12-h light/12-h dark cycle and food and water were provided ad libitum.

Radiation.—P17 mice were anesthetized with an intraperitoneal (i.p.) injection of tribromoethanol (250 mg per kg; Sigma-Aldrich) before being placed in a lead shield. The shield was constructed with a hole that allowed the mice to be secured such that only the head was exposed to radiation. Mice received a single 8-Gy dose of radiation using a cesium-137 gamma irradiator, which is approximately equivalent to 18 Gy delivered in 2-Gy fractions, thus reflecting a clinically relevant radiation paradigm[56]. Following radiation, mice were placed back with their mother and recovered under a heat lamp. Control (non-irradiated) mice received the injection of anesthesia.

Drug administration.—Metformin (1,1-dimethylbiguanide hydrochloride; Sigma) was dissolved in sterile PBS, while PBS was used as the vehicle control. Mice were administered PBS or 200 mg per kg metformin daily via i.p. injection (P18-27) followed by surgical implantation of 7-d subcutaneous osmotic pumps containing either PBS or metformin (P28-42, Durect Corporation).

Neurosphere assay.—Mice were anesthetized with tribromoethanol (250 mg per kg) and killed by cervical dislocation. Brains were quickly removed and the SVZ was microdissected as described previously[13,57]. For DG dissections, brains were placed in 2% low-temperature-gelling agarose (Sigma) and frozen on ice for 25 min before generating vibratome sections (500 μm) from which the DG was microdissected, taking care to exclude any periventricular tissue, as described[5]. Both SVZ and DG microdissections were placed into an enzyme solution (trypsin (1.3 mg ml^{-1}), hyaluronidase (0.76 mg ml^{-1}), kynurenic acid (0.12 mg ml^{-1}); Sigma-Aldrich) in artificial cerebrospinal fluid (aCSF), incubated for 30 min at 37 °C and then centrifuged at 1,500g for 5 min. The supernatant was removed, and the pellet was resuspended in a trypsin inhibitor solution (0.67 mg ml^{-1} in SFM; Worthington Biochemical). Samples were triturated and centrifuged at 1,500*g* for 5 min. The supernatant was again removed, and the samples were resuspended in SFM. Samples were centrifuged at 1,500*g* for 3 min. Finally, the supernatant was removed, samples were resuspended in 1 ml SFM and cells were counted with a hemocytometer. Cells were plated in SFM in the presence of fibroblast growth factor (20 ng ml^{-1}; Gibco), epidermal growth factor (20 ng ml^{-1}; Peprotech) and heparin (2 μg ml^{-1}; Sigma-Aldrich) with metformin (1 or 10 μM) at a clonal density of 10 cells per μl (ref. [58]). Control cells were plated in the absence of metformin. Cultures were incubated at 37 °C for 7 d, after which the resulting spheres were counted (>80 μm; microscope at × 10 magnification).

Tissue collection.—For immunohistochemistry of tissue sections, mice were anesthetized with 250 mg per kg tribromoethanol and transcardially perfused with ice-cold PBS followed by 4% paraformaldehyde (PFA). Brains were postfixed in 4% PFA for 1 h before being stored in 20% sucrose cryoprotectant solution and frozen. Brains were sectioned (20 μm; 200 μm apart) and frozen at −20 °C until use.

Immunohistochemistry.—For in vivo experiments, slides were defrosted before being rehydrated with PBS. Antigen retrieval was performed by incubating the sections in citrate buffer at 95 °C for 15 min. Slides were then cooled and incubated in 5% normal goat serum (NGS) in 0.03% Triton X-100 for 1 h at room temperature followed by incubation with primary antibody (mouse anti-DCX; 1:200 dilution in 5% NGS in 0.03% Triton X-100) at 4 °C overnight. The following day, slides were incubated with secondary antibody (donkey anti-mouse Alexa Fluor 568; 1:400 dilution) for 1 h at room temperature. Finally, the slides were incubated with DAPI (1:10,000 dilution) in PBS for 10 min at room temperature and then washed three times in PBS and coverslipped with Vectamount mounting medium (Vector). Images of the DG and SVZ were taken at ×20 magnification using a Zeiss microscope (Axiovert 200M, Zeiss), and DCX^+ cells were counted.

Behavioral assays.—Mice were tested at P43. Animals were acclimated to the behavioral testing suite for at least 10 min before the following tests were performed[59]. For all mouse behavioral assays, path length, velocity and time spent in regions of interest were recorded using the Biobserve Viewer (Biobserve).

Y maze.: The Y maze consisted of three identical arms, each 38 cm × 7.6 cm × 12.7 cm (length × width × height), connected at the center of the apparatus with 120 degrees between

each pair of adjacent arms (San Diego Instruments). Mice were placed into a randomly assigned arm of the Y maze and allowed to explore freely for 8 min. The spontaneous alternation performance (SAP) was measured as the percentage of time that the mice visited all three arms in sequence.

Open field.: A white opaque Plexiglas arena (62 cm × 40.5 cm × 23 cm (length × width × height)) was used for the open-field task. Mice were placed into an empty open arena and allowed to explore for 10 min. The path length, percentage of time that the mice were active and velocity were assessed for locomotor activity. The open-field test also served as an acclimation for the novel place recognition test.

Novel place recognition.: On the day after acclimation to the arena (62 cm × 40.5 cm × 23 cm (length × width × height)) in the open-field test, mice were familiarized with two identical objects placed in two corners of the arena for 10 min (exposure). The following day, one of these objects was moved to a novel location (diagonal to the original corner) and mice were allowed to explore for 5 min (testing). The proportion of time that mice spent exploring the object in the novel location was measured.

Elevated plus maze.: The elevated plus maze consisted of four arms (each 30.5 cm × 5 cm), meeting at a 5 cm × 5 cm intersection, with 90 degrees between each pair of adjacent arms. Two of the opposing arms had 15.25-cm walls, while the other two arms had no walls (San Diego Instruments). Mice were placed in the center of the elevated plus maze, with two open and two closed arms, and allowed to explore for 10 min. The percentage of time that mice spent in the open arms was measured.

Quantification and statistical analysis.—All preclinical data were analyzed using GraphPad Prism version 6 software. An unpaired Student's *t* test was used for all comparisons between two groups. For multiple comparisons, including the immunohistochemistry and behavioral assays, one-way ANOVA with Tukey's test was used. A *P* value less than 0.05 was considered statistically significant.

Pilot clinical trial.

Trial design.—A placebo-controlled, double-blind crossover design was used. Participants were randomly assigned to complete 12-week cycles of metformin (A) and placebo (B) in either an AB or BA sequence. At the point of crossover, there was a 10-week washout period in which neither group received any study pills (see Fig. 1a for the trial schema). We used a 10-week washout period on the basis of the pharmacokinetics of metformin as well as estimates of how long the effects of stimulation of endogenous NPCs by metformin may continue in the brain. As there are few data regarding this activation, we elected to use a relatively long washout period of 10 weeks. The study was reviewed and approved by Health Canada and the Research Ethics Board at the Hospital for Sick Children (REB#1000039383).

Participants.—The trial was conducted at the Hospital for Sick Children from March 2014 to December 2017. Information letters were mailed to the families of eligible patients, as

well as a brochure providing a brief synopsis of the study, including information regarding the purpose of the study, eligibility criteria, study visits and reimbursement. Eligible participants were identified from a Neuro-Oncology Program database using the following inclusion criteria: (1) between the ages of 5 and 21 years at the time of consent, (2) treated with cranial or cranial-spinal radiation for a brain tumor, (3) declared English as their native language or had at least 2 years of schooling in English at the time of their baseline assessment, (4) were diagnosed with a brain tumor at least 2 years before the start of the trial, (5) not receiving any active treatment, (6) 15 years or less from the time of administration of cranial or cranial-spinal radiation at the time of the trial, (7) females of childbearing potential must have had a negative pregnancy test result and agreed to use a medically acceptable method of contraception throughout the entire study period and for 30 d after the last dose of the study drug, (8) met criteria for adequate organ function (both renal and liver) and (9) informed consent provided either directly from the participant or from a legal guardian with participant assent.

Participants were not eligible if they met any of the following exclusion criteriaP (1) receiving palliative care, (2) unable to participate in neuroimaging without sedation, (3) unable to swallow pills, (4) unstable and/or insulin-dependent (type 1) diabetes, (5) diagnosed with acute or chronic metabolic acidosis and/or lactic acidosis, (6) known to have a history of congestive heart failure requiring pharmacologic treatment, (7) known to have a history of renal disease or renal dysfunction or abnormal creatinine clearance, (8) known hypersensitivity to metformin hydrochloride, (9) any female patient or partner who had reached menarche and male patients who were not willing to use an effective method of contraception or (10) pregnant or lactating and did not agree to stop breastfeeding while receiving the study pills.

One hundred and thirty patients were prescreened and, of these, 114 were potentially eligible. Twenty-four participants provided informed consent (or parental consent with participant assent, where applicable) and were enrolled, for a recruitment rate of 21% (see Extended Data Fig. 4 for the consort diagram). Consent was obtained by a healthcare practitioner not part of the research team. Although a prespecified sample of 30 participants and expected recruitment rate of 25% were not reached, the trial was discontinued as we reached saturation within the sample of identified eligible participants and it was not feasible to prolong the trial so that newly diagnosed individuals could be assessed for eligibility. The primary reasons patients/parents declined participation included (1) concerns regarding taking additional medication, side effects or medical procedures (34%); (2) logistical concerns for the family regarding research participation (that is, timing issues; too many visits; travel; time missed from school/work) (33%) and (3) no interest in research participation or no response (19%). The first participant was enrolled on 13 June 2014 and the last participant completed the trial on 15 December 2017. We compared the medical and demographic characteristics of eligible participants who did ($n = 24$) and did not ($n = 90$) participate in the trial on a number of relevant medical variables. We found no differences in mean age at diagnosis ($F_{(1,110)} = 0.27$, $P = 0.60$, 6.85 versus 7.34 years), sex ($\chi^2_{(1)} = 0.07$, $P = 0.80$, male = 58% versus 61%; female = 42% versus 39%), tumor location ($\chi^2_{(1)} = 0.82$, $P = 0.37$, supratentorial = 42% versus 32%; subtentorial/posterior fossa = 58% versus 68%) or radiation treatment ($\chi^2_{(1)} = 1.04$, $P = 0.31$, cranial-spinal = 58% versus 47%; focal/

ventricular = 42% versus 53%) between eligible patients who did and did not participate in the trial. Although the overall distribution of tumor type was not different between the groups, there were fewer ependymoma and more other tumor diagnoses for the trial participants ($\chi^2_{(4)} = 4.91$, $P = 0.30$, medulloblastoma = 50% versus 38%; ependymoma = 8% versus 28%; germ cell = 12.5% versus 13.5%; other tumors (that is, atypical teratoid/rhabdoid tumor, craniopharygioma, pineoblastoma, hemangioblastoma, sarcoma, astroblastoma) = 29% versus 19%).

Metformin and placebo.—The dose and schedule of administration were based on safety and toxicity data obtained from previous use of metformin in pediatric populations[7-11] and animal studies evaluating metformin-related behavioral and structural changes in the brain[4,13]. For each 12-week treatment cycle, metformin and placebo doses were 500 mg m^{-2} per day p.o. given in one or two divided doses for 1 week. If there were no side effects, the dose was increased to 1,000 mg m^{-2} per day p.o. given in two divided doses for the rest of the 12-week treatment cycle. Doses were rounded to increments of half tablets and based on body surface area (BSA) using the Mostellar calculation, at the beginning of each treatment cycle. Participants received a minimum 12-week supply of blinded study pills as an outpatient prescription filled by the Hospital for Sick Children Research Support Pharmacy. Participants were provided a 12-week medication diary for each cycle, in which they or their parent(s) were asked to record information regarding the time the study pills were taken, the dose (that is, number of pills) taken, the reason for any missed doses and any side effects experienced. In addition, participants received a phone call from the study coordinator during week 6 and week 28 to support adherence. The pill bottles were returned with any remaining study pills to the study coordinator at the end of each 12-week treatment cycle.

The investigational agent was a commercial supply of 500-mg oral white round film-coated pills (brand name Glucophage) from Sanofi Canada. Matching white round pills containing inactive ingredients with a score marking on one face to match the active pills were manufactured for this trial by Valeant Pharmaceuticals, Canada.

Safety assessment.—Lactic acidosis is the most serious complication of metformin, usually in the context of overdose, although this can sometimes occur in the context of renal failure or severe hepatic dysfunction; therefore, normal kidney and liver function was ensured before participation[60]. The youngest age that metformin has been prescribed is 2 years[61]. Overall, no serious complications have been reported with use of metformin in the pediatric population. To monitor safety, complete blood counts, blood differentials, platelets, liver function tests, and serum creatinine and lactate levels were measured at all six study visits (baseline, end of week 1, end of cycle 1 (week 12), before the start of cycle 2 (week 22), end of week 23 and end of cycle 2 (week 34)). Metformin was discontinued if lactate levels were above normal values (lactate levels > 5 mmol l^{-1}) and assessed to be clinically relevant by a study team physician. One participant had clinically elevated liver function at baseline. This participant was monitored by their family physician for 3 weeks, after which time they were approved to start the trial. A second participant had clinically elevated alanine aminotransferase (ALT), white blood cell count and creatinine at week 23 (1 week on 500 mg m^{-2}), which after unblinding was determined to be during treatment with

placebo. They were maintained on half the placebo dose and monitored with repeated bloodwork with additional tests to explore the possibility of dehydration for 4 d. All parameters normalized, and the physician approved the participant to increase to the full dose.

Adverse events were assessed using an 'Adverse Events' case report form that was completed by a study team physician at each clinic visit. The study team physician assessed the following for each adverse event: (1) the grade according to the National Cancer Institute Common Terminology Criteria for Adverse Events (CTCAE) v.4 (mild; moderate; severe; life-threatening; fatal), (2) whether it was expected (yes; no), (3) whether it was serious (yes; no) and (4) whether the adverse event could be attributed to the investigational agent (metformin) (no relation; unlikely; possible; probable; definite). All randomized participants were followed and evaluated for outcome, even if the study medication was interrupted or not given. Because of the known safety profile of this medication, a data safety monitoring board was not used. Relevant adverse events were reported and managed according to the Hospital for Sick Children's adverse event reporting requirements and standard clinical management practices and according to Health Canada requirements. Safety was assessed by monitoring adverse events previously reported with metformin. These assessments were administered by a study team physician at every visit.

Feasibility assessment.—Recruitment rate was calculated as the percentage of participants enrolled as a function of the total number of individuals eligible. Medication adherence was calculated by subtracting the number of pills returned at the end of each cycle from the total number of pills given at the start of the cycle divided by the number of pills the participant was expected to have taken. Adherence to cognitive testing and MRI was defined as a participant completing the required assessments. Participants were given a score of 1 if they completed testing and a score of 0 if they were unable to complete testing. The overall percentage of adherence was calculated as the number of participants who successfully completed testing divided by the total number of participants in the study (Fig. 3b).

Cognitive assessment.—Initially, cognitive testing and neuroimaging data were acquired at three time points: at baseline, following the 10-week washout period (week 22) and at the end of the trial at ~34 weeks (Fig. 1c, cognitive outcomes, and Fig. 1d, MRI outcomes). After commencement of the pilot trial, we realized that the timing of the post-washout outcome assessment was not optimal for testing potential metformin effects from the first cycle. Consequently, we submitted an amendment to revise the study protocol to include an additional assessment immediately after the first cycle at ~12 weeks. When this amendment was approved by the required regulatory and institutional bodies, cognitive testing and neuroimaging were conducted at the following four time points for all remaining participants: study entry (baseline 1), at ~12 weeks (outcome 1), after the 10-week washout period at 22 weeks (baseline 2) and at the end of the trial at ~34 weeks (outcome 2).

Declarative memory.: The CAVLT-2 was used to assess auditory verbal memory in participants younger than 18 years[34]. For participants who were 18 years or older, the RAVLT was used[35]. In both tests, participants were asked to learn and recall a list of words

presented over a series of five trials. Measures of level of learning, interference, immediate recall and delayed recall (after a ~20-min delay) were obtained. The CAVLT-2 and RAVLT have good concurrent validity[62].

NIH Toolbox.: Visual-spatial and working memory were assessed using subtests from the NIH Toolbox (http://www.nihtoolbox.org)[33]. The PSM was used to measure visual-spatial memory, and the LSWM was used to assess auditory working memory.

The Cambridge Neuropsychological Test Automated Battery.: The CANTAB (cognitive assessment software; Cambridge Cognition, 2018; https://www.cantab.com/) is a well-validated computerized tool that has been used with multiple pediatric populations[36]. We used subtests measuring attention (Rapid Visual Information Processing (RVP), Match to Sample (MTS)), processing speed (Simple Reaction Time (SRT), Choice Reaction Time (CRT)) and short-term memory (Delayed Matching to Sample (DMS)). Participants' accuracy and reaction time (correct trials only) were calculated for each subtest and were averaged across all subtests to provide a composite value of accuracy and latency for responding, as we have reported previously[63].

MRI acquisition protocols and image processing.—All images were acquired at the Hospital for Sick Children on either a (1) Siemens Tim Trio 3T MRI scanner with a 12-channel head coil that was upgraded to a Siemens Prisma Fit scanner with a 20-channel head coil in the summer of 2016 (Siemens Canada) or (2) GE Signa HDxt 1.5T MRI scanner with an 8-channel head coil (GE Healthcare). We were unable to scan two participants at 3 T owing to safety reasons associated with the presence of surgical implant/hardware. These two participants were scanned using the 1.5T scanner. We acquired an anatomical T1-weighted image, DKI (on the 3 T scanner only) and pulsed ASL (Fig. 1d). On the 3T scanner, the T1 protocol included three-dimensional (3D) T1 sagittal MPRAGE Grappa 2 acquisition (TI = 900 ms; TE/TR = 2.96/2,300 m; 192 contiguous slices; flip angle = 9°; matrix = 256 × 256; field of view (FOV) = 256 × 256 mm^2; voxel size = 1 mm isotropic). For the 1.5 T scanner, we acquired a 3D T1 sagittal fast spoiled, gradient-echo, inversion recovery-prepared sequence (TI = 300 ms; TE/TR = 4.2/9.188 ms; 150 contiguous slices; flip angle = 20°; matrix = 256 × 256; FOV = 256 × 256 mm^2; voxel size = 1 mm isotropic). DKI was acquired on only the 3T scanner, using an echo-planar imaging two-dimensional (2D EPI) Grappa 2 sequence performed in the axial plane with 30 directions, three b values (0, 1,000 and 2,000 s mm^{-2}) and the following parameters: TE/TR = 101/6,800 ms; 50 slices; flip angle = 90°; matrix = 82 × 82; FOV = 222 × 222 mm^2; voxel size = 2.7 mm isotropic. Pulsed ASL (PICORE QT2) images were acquired with a 2D EPI readout with the following details: TE/TR = 11/2,500 ms; TI1/2 = 700/1,800 ms; voxel size = 1.5 × 1.5 mm^2 interpolated to 0.75 × 0.75 × 5 mm^3 and matrix size = 64 × 64 interpolated to 128 × 128. A total of 50 control–label pairs and an M0 calibration image were collected. DKI is a clinically feasible extension of diffusion tensor imaging sensitive to tissue environment at the cellular scale.

Delineating the corpus callosum and hippocampus.: Automated segmentation of the T1-weighted images was performed using FreeSurfer version 6.0 (ref. [64]). First, the brain was

removed from the skull, and intensity normalization and segmentation of the brain into gray matter, white matter and cerebrospinal fluid was conducted. Quality control was performed to ensure the accuracy of the brain extraction and white matter labeling. Manual editing of the white matter surface was required in approximately 44% of the brain images. Lastly, corpus callosum and hippocampal segmentations were extracted. This process created a neuroanatomical label for each location[65]. This parcellation used both geometric and neuroanatomical information based on previously generated atlases: the MNI305 atlas was used as a reference for the neuroanatomical labeling[65]. To extract values obtained from DKI within substructures of the corpus callosum, five regions were analyzed (anterior, middle anterior, central, middle posterior and posterior corpus callosum).

Diffusion imaging analyses.: The DESIGNER toolkit was used to perform diffusion preprocessing[66], including denoising[67,68], Gibbs artifact correction[69], Rician bias correction, eddy current and motion correction[70] and signal outlier detection[71], using MRtrix3, FMRIB Software Library (FSL) and MATLAB version R2015b. The WMTI model was used to interpret DKI in terms of the intra- and extra-axonal compartments[38], which allows for quantification of the following myelin-sensitive WMTI metrics: AWF and extra-axonal radial diffusivity ($D_{e,\perp}$[39]. Using the DESIGNER toolkit, AWF and $D_{e,\perp}$ were calculated from the kurtosis tensor and image quality was evaluated on the basis of the presence of nonphysical outlier voxels in outcome parametric maps[38].

To conduct analyses of the corpus callosum, the b0 was registered to each participant's T1-weighted image using an affine transformation within ANTS[72]. This transformation was then applied to AWF and $D_{e,\perp}$ maps. Mean AWF and $D_{e,\perp}$ values for the corpus callosum were extracted, weighting the means by the volume of the five subregions (anterior, middle anterior, central, middle posterior and posterior corpus callosum) to account for regional volume differences.

We also conducted voxel-wise analyses of the AWF and $D_{e,\perp}$ across the entire brain using TBSS following a longitudinal approach[40,73]. First, halfway registrations between pre- and post-metformin treatment assessments were generated and averaged to create a study-specific midway mean fractional anisotropy (FA) skeleton map. This was thresholded at FA > 0.20 to only include fiber tracts with larger anisotropy. For comparisons across treatment conditions, individual difference maps for AWF and $D_{e,\perp}$ (after metformin minus before metformin) were projected onto the skeleton and tested for voxels where the change was significantly different from zero using threshold-free cluster enhancement (TFCE). For these analyses, the null distribution of the cluster size statistic was built up over 5,000 random permutations. Cluster size was thresholded at $P < 0.05$, which is family-wise fully corrected for multiple comparisons across space.

Hippocampal blood flow analyses.: Pulsed ASL data were processed using tools within FSL[74,75]. ASL volumes were linearly registered to a reference volume, a mean control image. Control and label images underwent motion correction, difference images were calculated and scans with excessive head motion were removed[76]. CBF values were calculated for each voxel[77,78]. Structural T1-weighted images were linearly co-registered to

the ASL image, and hippocampal masks from FSL were transformed and aligned with the CBF image. Mean CBF values were extracted from the left and right hippocampi.

Missing data.

Missing cognitive data.—The CANTAB RVP was not acquired across three of the four assessments in a single participant owing to task difficulty. In a second participant, the DMS was not acquired owing to time constraints. Further, measures from the NIH Toolbox were not obtained for a single assessment time point in a different participant owing to technical difficulties with the program.

Missing imaging data.—One participant discontinued the study after the first baseline assessment and no further imaging was acquired. Further, DKI and ASL sequences were not acquired in two participants who had to be scanned at 1.5 T owing to scanner limitations. Furthermore, AWF and $D_{e,\perp}$ values within the corpus callosum were not achieved for eight scans across three participants owing to poor segmentation of white matter within the T1 or poor registration with DKI. Likewise, CBF values were not obtained for a single participant owing to poor segmentation of the hippocampus. Finally, ASL was not obtained for a single session at 3 T in a further participant owing to early termination of the scanning session.

Randomization and blinding.

Participants were randomly assigned to the two sequence groups (AB or BA) using block 4, 1:1 randomization. The Research Support Pharmacy at the Hospital for Sick Children designed and maintained the Master Randomization Table. All others involved, including participants and their families, healthcare providers and research team members, were blind to treatment assignment, which was not revealed until all participants had completed the trial and data processing and scoring were completed.

Quantification and statistical analysis.

Sample size.—We previously documented a large effect size (that is, 0.40–1.45) for cognitive and white matter changes in patients with a brain tumor treated with radiation as compared to healthy children[22,23]. A sample size of 30 is sufficient to detect a large effect size for group comparisons with two groups with a power of 0.80 at an alpha level of 0.01 (ref. [79]). Hence, we determined a sample of 30 participants as reasonable for the pilot trial to evaluate safety and feasibility and to conduct exploratory analyses of cognitive and imaging measures.

Statistical analyses.

Analysis of variance or chi-squared analyses were used to compare the sequence groups (AB versus BA) at baseline on demographic and medical information.

With the addition of an outcome assessment time point, we modified our prespecified analyses of the cognitive and MRI outcomes after the trial had ended. However, the final analytic plan was developed independently by a consulting biostatistician from the Hospital for Sick Children's Clinical Trials Support Unit. We provided this consultant, who was not part of the study team and who was blind to the trial data, with our final trial design and

outcome assessment time points and they designed the following plan. Separate general linear mixed models were used for each cognitive and MRI measure with two sets of outcomes (outcomes 1 and 2 corresponding to the end of the first and second 12-week treatment cycles, respectively). We examined the fixed effects of cycle (first versus second 12-week treatment cycle), treatment (metformin versus placebo) and sequence (metformin first, placebo second (AB) versus placebo first, metformin second (BA)) on raw test scores (accuracy and latency data) in separate models for the cognitive measures, DKI indices (AWF and $D_{e,\perp}$ within the corpus callosum and voxel-wise across white matter, and CBF within the hippocampus. All these measures are continuous numerical variables. The cycle variable separated the two cycles from each other and was included to test for the effects of time on outcome measures, including practice effects for cognitive measures and brain maturation for imaging across the course of the study. The treatment variable was included to test the effects of metformin versus placebo. Finally, the sequence variable tested the interaction between cycle and treatment, that is, the residual carry-over effects in cycle 2. Baseline observations (baseline 1 and 2 corresponding to the start of the first and second 12-week treatment cycles, respectively), each of which corresponded to one outcome observation, were included as a fixed covariate. A random effect for participant was added to each model as an independent variable to account for the correlation between the two independent baseline and outcome observations from each participant. Further, for each outcome measure, we conducted a series of further models where any medical characteristic that differed significantly between sequence groups at baseline was included as a covariate in separate models. These models were conducted separately for each medical covariate. All models were corrected for multiple comparisons (FDR $q < 0.10$). Statistical analyses were conducted using SPSS or R Studio.

Extended Data

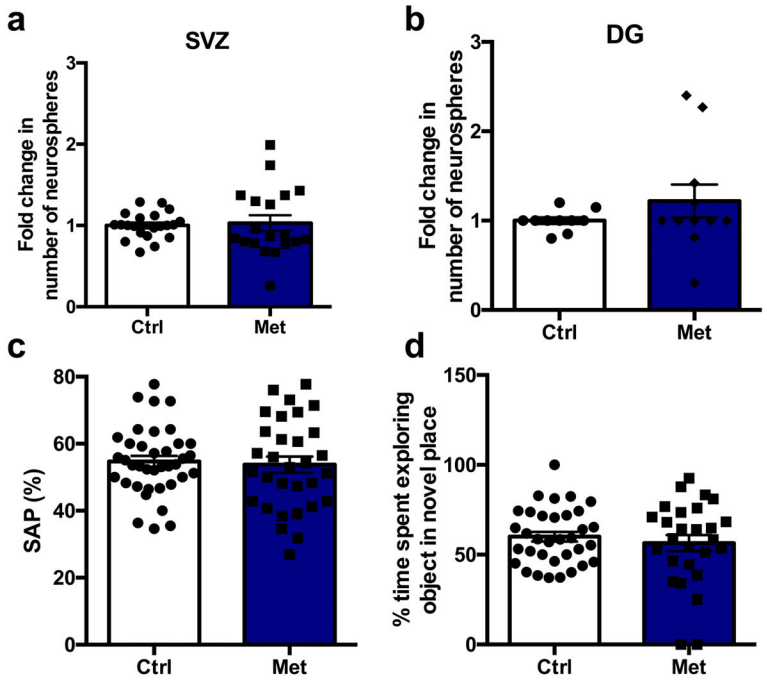

Extended Data Fig. 1 | Metformin in the absence of injury has no significant effect on the number of neurospheres or on behavioural assays.

a, **b**, Fold change in the number of neurospheres from the (**a**) SVZ (n = 21 Ctrl, 19 Met mice over 10 independent experiments; t(38) = 0.10, p = 0.92) and (**b**) DG (n = 12 Ctrl, 10 Met mice over 5 independent experiments; t(20) = 0.90, p = 0.38) 5 weeks post-radiation. **c**, Spontaneous alternation performance measured using the Y maze at P43 (n = 38 Ctrl, 31 Met mice over 14 independent experiments; t(67) = 0.34, p = 0.74). **d**, Percentage of time spent exploring objects in a novel place measured using the novel place recognition task from P44-46 (n = 34 Ctrl, 27 Met over 13 independent experiments; t(59) = 0.70, p = 0.48). Two-sided unpaired t-test was used for all analyses. Data is presented as mean ± SEM.

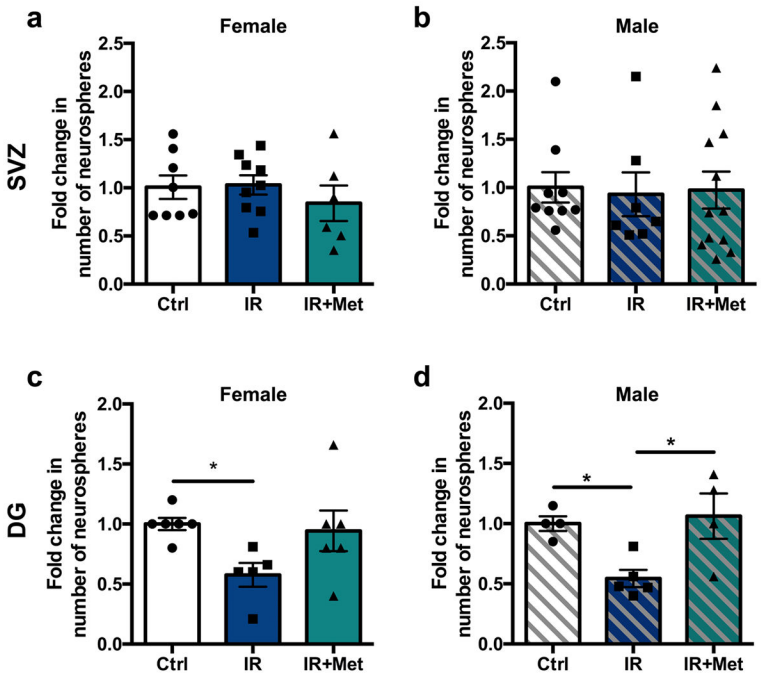

Extended Data Fig. 2 |. Metformin's effects on NSC pool recovery following juvenile cranial radiation are not sex-dependent.

a, **b**, Fold change in the number of neurospheres from the SVZ 5 weeks post-radiation in (**a**) females (n = 8 Ctrl, 9 IR, 6 IR + Met mice over 6 independent experiments; $F(2,20) = 0.56$, $p = 0.58$) and (**b**) males (n = 9 Ctrl, 7 IR, 12 IR+Met mice over 6 independent experiments; $F(2,25) = 0.03$, $p = 0.97$). (c-d) Fold change in the number of neurospheres from the DG 5 weeks post-radiation in (**c**) females (n = 6 Ctrl, 5 IR, 6 IR+Met mice over 4 independent experiments; $F(2,14) = 3.47$, $p = 0.06$; Ctrl vs. IR, $p = 0.0496$) and (**d**) males (n = 4 Ctrl, 5 IR, 4 IR+Met over 4 independent experiments; $F(2,10) = 6.47$, $p = 0.02$; Ctrl vs. IR, $p = 0.04$; IR vs. IR+Met, $p = 0.02$). *$p < 0.05$, one-way ANOVA with Tukey's test was used for all analyses. Data is presented as mean ± SEM.

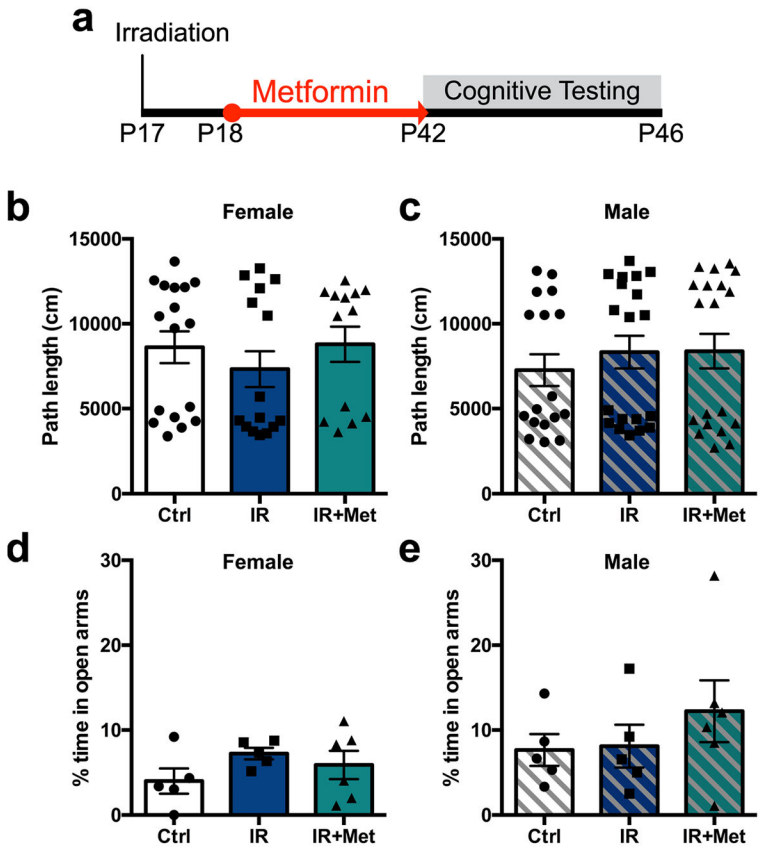

Extended Data Fig. 3 |. Cranial radiation does not lead to impairments in the open field test or in the elevated plus maze.

a, Experimental paradigm. IR=cranial radiation. **b**, **c**, Path length travelled over 10 minutes in an open arena by (**b**) females (n = 17 Ctrl, 15 IR, 13 IR+Met mice over 13 independent experiments; $F(2,42) = 0.62$, $p = 0.54$) and (**c**) males (n = 17 Ctrl, 19 IR, 19 IR+Met mice over 13 independent experiments; $F(2,52) = 0.40$, $p = 0.67$). **d**, **e**, Percentage of time spent in the open arms of the elevated plus maze over 10 minutes by (**d**) females (n = 5 Ctrl, 5 IR, 6 IR+Met mice over 4 independent experiments; $F(2,13) = 1.26$, $p = 0.32$) and (**e**) males (n = 5 Ctrl, 5 IR, 6 IR+Met mice over 4 independent experiments; $F(2,13) = 0.78$, $p = 0.48$). One-way ANOVA with Tukey's test was used for all analyses. Data is presented as mean ± SEM.

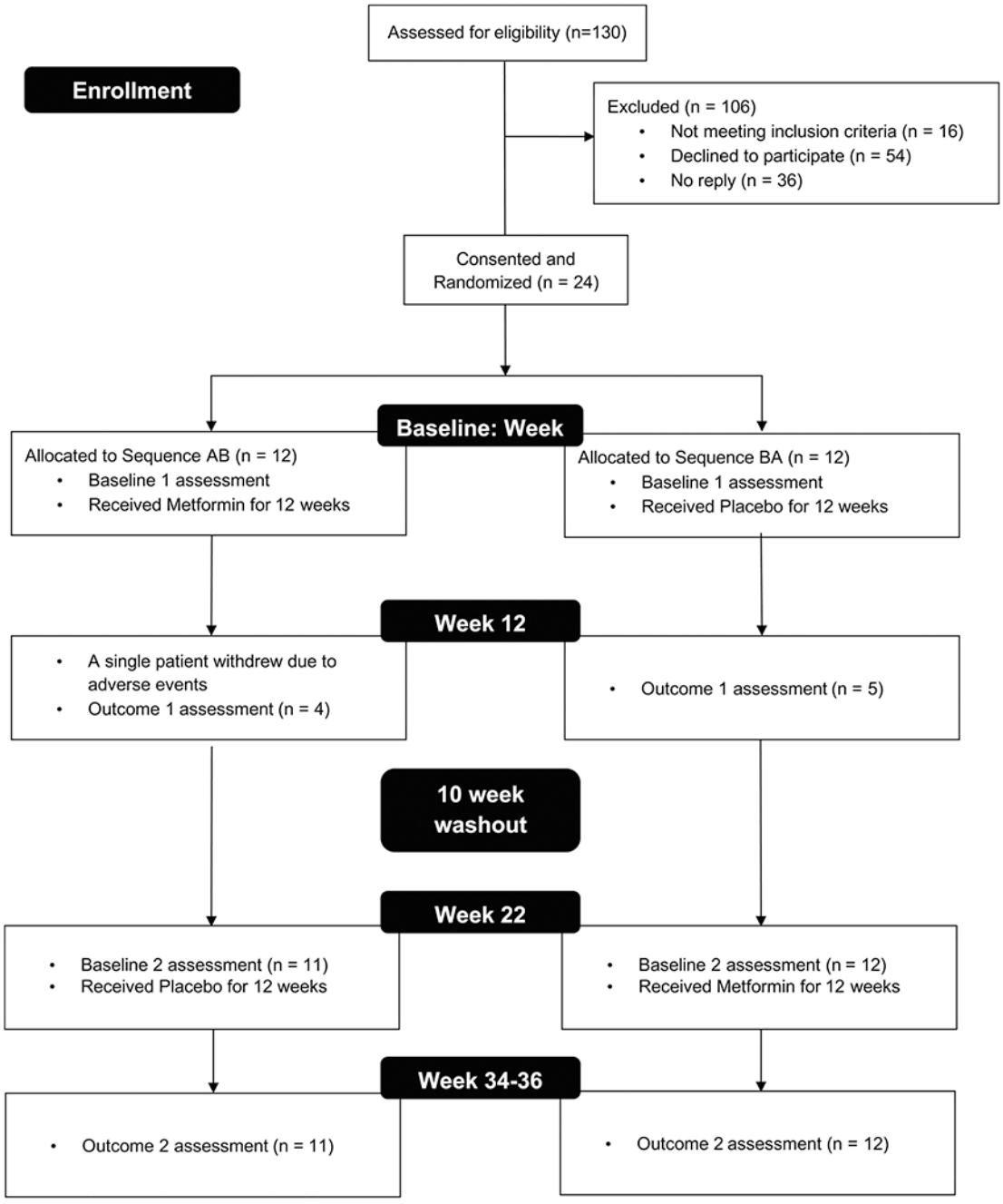

Extended Data Fig. 4 |. Consort table.

Eligible participants were identified via database review. Randomization was conducted by the Research Support Pharmacy and all research personnel remained blind to treatment assignment until all participants had completed the trial and data processing and scoring was completed. Initially, due to the pilot nature of the trial, neuroimaging and neuropsychological assessments were acquired at three time points (Baseline 1 and 2; Outcome 2). With an amendment to the study protocol, subsequent participants were assessed at four time points (Baseline 1 and 2; Outcome 1 and 2). Therefore, fewer Outcome 1 than Outcome 2 data points were acquired. Linear mixed modeling can be used in the

context of such missing data. The single participant who consented but did not complete the trial was not included in the analyses.

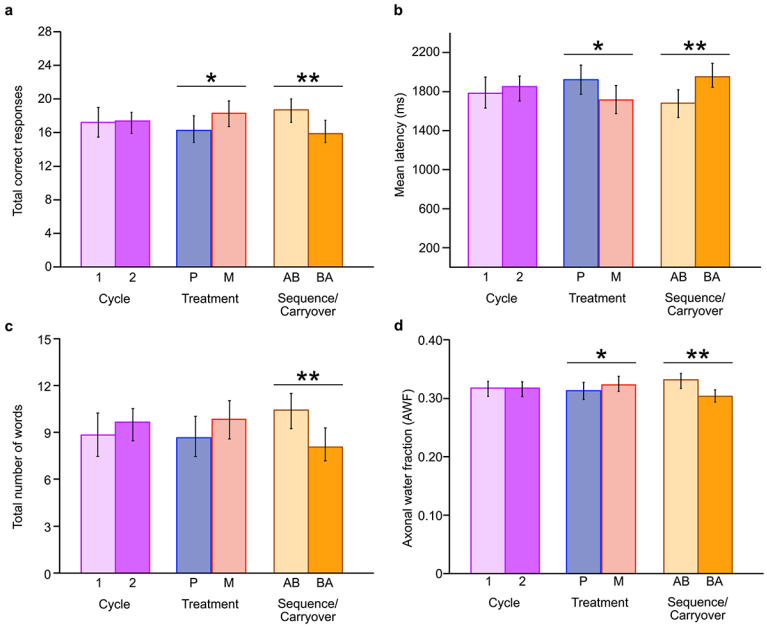

Extended Data Fig. 5 |. Estimated marginal means for linear mixed models of cognitive and WMTI outcomes.

Data are presented as estimated marginal means from seperate general linear mixed models (two sided) with two sets of outcomes (Outcome 1 and 2 corresponding to the end of the first and second 12-week treatment cycles, respectively). We examined the fixed effects of cycle (the first versus second 12-week treatment cycle), treatment (metformin versus placebo), and sequence (metformin first, placebo second [AB] versus placebo first, metformin second [BA]). Bar graphs show estimated means+/− SEMs from the following model: Outcome measure = cycle + treatment + sequence + covariate (Baseline measure) + (1| participant ID+**ε**, where cycle, treatment, and sequence are independent fixed effects and where the measures are: **a**) total correct on the LSWM (n = 23); **b**) CANTAB mean latency (n = 22); **c**) total number of words recall for immediate recall (n = 23); and **d**) AWF. Standard error bars are shown for each estimated mean. All models were corrected for multiple comparisons (False Discovery Rate (FDR) q < .10): * p < 0.05, ** q < 0.10 from the linear mixed models (Panel a-c, qs = 0.09; Panel d, q = 0.08).

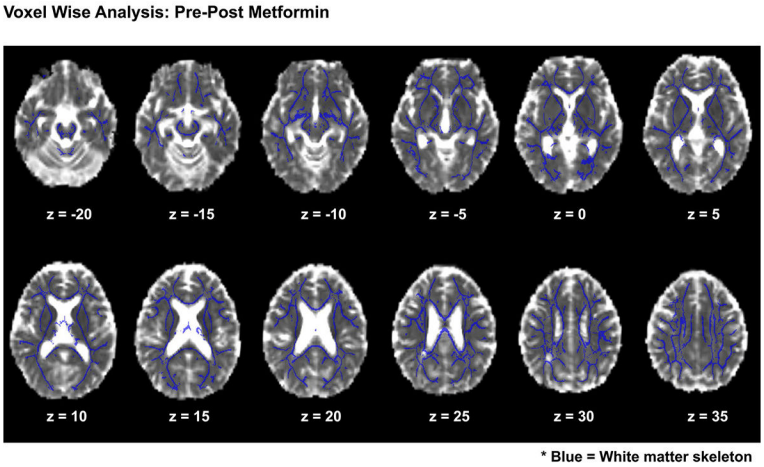

Extended Data Fig. 6 |. Voxel wise analyses of treatment effects.

We used a longitudinal voxel wise approach to test for clusters of significant changes in AWF and $D_{e,\perp}$ following metformin in all participants using Tract Based Spatial Statistics (TBSS). For 2 sided comparisons across treatment conditions, individual difference maps for AWF and $D_{e,\perp}$ (post-metformin minus pre-metformin) were projected onto the skeleton and tested for voxels where change was significantly different from zero using threshold-free cluster enhancement (TFCE). For these analyses, the null distribution of the cluster-size statistic was built up over 5000 random permutations. Cluster size was thresholded at $P < 0.05$, which is family wise fully corrected for multiple comparisons across space. Images are presented in the axial frame in radiological convention within Montreal Neurological Institute (MNI) Z-coordinates. The white matter skeleton is displayed in blue. No significant clusters of change were evident for AWF ($p = .90$) or $D_{e,l}$ ($p = .47$) across the white matter skeleton.

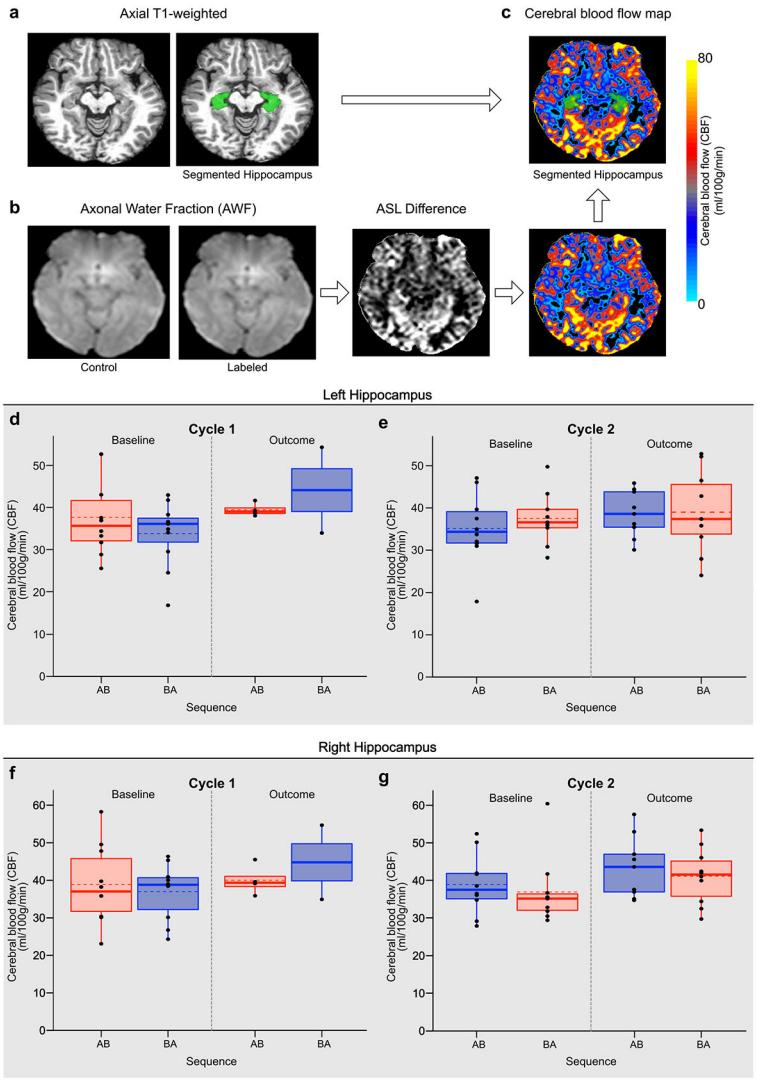

Extended Data Fig. 7 |. Arterial Spin Labelling and Cerebral Blood Flow within the Hippocampus as a function of cycle, treatment, and sequence effects for the right and left hippocampi and adjusted for baseline hippocampal CBF.

a, Axial T1-weighted image with FreeSurfer hippocampus segmentation shown. **b**, PASL image processing pipeline shown in the axial plane, including PASL Control, PASL Labeled image, Perfusion weighted Image and Cerebral Blood Flow Map. **c**, Segmented hippocampi registered to the CBF map. Boxplots showing all data points at baseline and outcome assessment with the mean (dashed line) and median (solid line) sequence group observations for CBF (ml/100 g/min) for: the left hippocampus at **d**) Cycle 1 and **e**) Cycle 2; and the right hippocampus at **f**) Cycle 1 and g) Cycle 2. Metformin treatment condition is shown in red and placebo in blue. The upper and lower limits of the box plots are the third and first quartiles (75th and 25th percentile), respectively. The whiskers extend up to 1.5 times the interquartile range from the top (bottom) of the box to the furthest datum within that distance: Data beyond this distance are represented individually as points.

Acknowledgements

We wish to thank A. Willan, Clinical Trials Methodologist, Ontario Child Health Support Unit, Research Institute, The Hospital for Sick Children, for consulting on and developing our analytic approach while blind to the trial data. We also wish to thank the research personnel and clinical staff who made this trial possible, particularly V. Ramaswamy, U. Bartels, U. Tabori and A. Huang, as well as N. Sarvaria, D. Thomas, E. Barlev, J. Dutton, J. Gammon, L. Lauer, A. Decker, A. Ferkul, D. McRae, T. Rayner, R. Weiss and M. Lalancette. We would also like to thank J. Wang, D. Kaplan and P. Frankland for frequent discussions and advice during the course of this work. Finally, we wish to thank J. Tseng for her technical support in improving the presentation of our figures. This work was supported by grants from Brain Canada (F.D.M., D.J.M., C.M.M.), the Stem Cell Network (F.D.M., D.J.M., C.M.M.), the Ontario Institute for Regenerative Medicine (F.D.M., D.J.M., C.M.M.), Medicine By Design (CFREF), and the Garron Family Cancer Centre (D.J.M., E.B.). R.M.R. was supported by a CIHR graduate student fellowship.

Data availability

Requests for data related to the rodent studies should be directed to, and will be fulfilled by, senior corresponding author C.M.M. Requests for resources from the pilot clinical trial, including a copy of the trial protocol and aggregate data, should be directed to, and will be fulfilled by, senior corresponding author D.J.M. Data from individual participants in the pilot trial are not available owing to privacy and confidentiality and participants did not explicitly consent for their data to be shared.

References

1. Miller FD & Kaplan DR Mobilizing endogenous stem cells for repair and regeneration: are we there yet? Cell Stem Cell 10, 650–652 (2012). [PubMed: 22704501]
2. Ming GL & Song H Adult neurogenesis in the mammalian brain: significant answers and significant questions. Neuron 70, 687–702 (2011). [PubMed: 21609825]
3. Lazarini F & Lledo PM Is adult neurogenesis essential for olfaction? Trends Neurosci. 34, 20–30 (2011). [PubMed: 20980064]
4. Wang J et al. Metformin activates an atypical PKC–CBP pathway to promote neurogenesis and enhance spatial memory formation. Cell Stem Cell 11, 23–35 (2012). [PubMed: 22770240]
5. Chow A & Morshead CM Cyclosporin A enhances neurogenesis in the dentate gyrus of the hippocampus. Stem Cell Res. 16, 79–87 (2016). [PubMed: 26720914]
6. Scafidi J et al. Intranasal epidermal growth factor treatment rescues neonatal brain injury. Nature 506, 230–234 (2014). [PubMed: 24390343]
7. Bridger T, MacDonald S, Baltzer F & Rodd C Randomized placebo-controlled trial of metformin for adolescents with polycystic ovary syndrome. Arch. Pediatr. Adolesc. Med 160, 241–246 (2006). [PubMed: 16520442]
8. Benavides S, Striet J, Germak J & Nahata MC Efficacy and safety of hypoglycemic drugs in children with type 2 diabetes mellitus. Pharmacotherapy 25, 803–809 (2005). [PubMed: 15927898]
9. Sun J, Wang Y, Zhang X & He H The effects of metformin on insulin resistance in overweight or obese children and adolescents: a PRISMA-compliant systematic review and meta-analysis of randomized controlled trials. Medicine 98, e14249 (2019). [PubMed: 30681616]
10. Bjornstad P et al. Metformin improves insulin sensitivity and vascular health in youth With type 1 diabetes mellitus. Circulation 138, 2895–2907 (2018). [PubMed: 30566007]
11. Anagnostou E et al. Metformin for treatment of overweight induced by atypical antipsychotic medication in young people with autism spectrum disorder: a randomized clinical trial. JAMA Psychiatry 73, 928–937 (2016). [PubMed: 27556593]
12. Wang J et al. CBP histone acetyltransferase activity regulates embryonic neural differentiation in the normal and Rubinstein–Taybi syndrome brain. Dev. Cell 18, 114–125 (2010). [PubMed: 20152182]

13. Dadwal P et al. Activating endogenous neural precursor cells using metformin leads to neural repair and functional recovery in a model of childhood brain injury. Stem Cell Rep. 5, 166–173 (2015).
14. Ruddy RM, Adams KV & Morshead CM Age- and sex-dependent effects of metformin on neural precursor cells and cognitive recovery in a model of neonatal stroke. Sci. Adv 5, eaax1912 (2019). [PubMed: 31535024]
15. Tanokashira D et al. Metformin treatment ameliorates diabetes-associated decline in hippocampal neurogenesis and memory via phosphorylation of insulin receptor substrate 1. FEBS Open Biol. 8, 1104–1118 (2018).
16. Ould-Brahim F et al. Metformin preconditioning of human induced pluripotent stem cell-derived neural stem cells promotes their engraftment and improves post-stroke regeneration and recovery. Stem Cells Dev. 27, 1085–1096 (2018). [PubMed: 29893190]
17. Monje ML, Mizumatsu S, Fike JR & Palmer TD Irradiation induces neural precursor-cell dysfunction. Nat. Med 8, 955–962 (2002). [PubMed: 12161748]
18. Monje ML, Toda H & Palmer TD Inflammatory blockade restores adult hippocampal neurogenesis. Science 302, 1760–1765 (2003). [PubMed: 14615545]
19. Redmond KJ, Mahone EM & Horska A Association between radiation dose to neuronal progenitor cell niches and temporal lobes and performance on neuropsychological testing in children: a prospective study. Neuro Oncol. 15, 1455 (2013). [PubMed: 24174569]
20. Roughton K, Kalm M & Blomgren K Sex-dependent differences in behavior and hippocampal neurogenesis after irradiation to the young mouse brain. Eur. J. Neurosci 36, 2763–2772 (2012). [PubMed: 22758785]
21. Riggs L et al. Changes to memory structures in children treated for posterior fossa tumors. J. Int. Neuropsychol. Soc 20, 168–180 (2014). [PubMed: 24460980]
22. Decker AL et al. Smaller hippocampal subfield volumes predict verbal associative memory in pediatric brain tumor survivors. Hippocampus 27, 1140–1154 (2017). [PubMed: 28667671]
23. Scantlebury N et al. White matter and information processing speed following treatment with cranial-spinal radiation for pediatric brain tumor. Neuropsychology 30, 425–438 (2016). [PubMed: 26752125]
24. Krull KR, Hardy KK, Kahalley LS, Schuitema I & Kesler SR Neurocognitive outcomes and interventions in long-term survivors of childhood cancer. J. Clin. Oncol 36, 2181–2189 (2018). [PubMed: 29874137]
25. Rola R et al. Radiation-induced impairment of hippocampal neurogenesis is associated with cognitive deficits in young mice. Exp. Neurol 188, 316–330 (2004). [PubMed: 15246832]
26. Fukuda A et al. Age-dependent sensitivity of the developing brain to irradiation is correlated with the number and vulnerability of progenitor cells. J. Neurochem 92, 569–584 (2005). [PubMed: 15659227]
27. Hellstrom NA, Bjork-Eriksson T, Blomgren K & Kuhn HG Differential recovery of neural stem cells in the subventricular zone and dentate gyrus after ionizing radiation. Stem Cells 27, 634–641 (2009). [PubMed: 19056908]
28. Ruddy RM, Derkach D, Dadwal P & Morshead CM Cranial irradiation in juvenile mice leads to early and sustained defects in the stem and progenitor cell pools and late cognitive impairments. Brain Res. 1727, 146548 (2019). [PubMed: 31715143]
29. Sorrells SF et al. Human hippocampal neurogenesis drops sharply in children to undetectable levels in adults. Nature 555, 377–381 (2018). [PubMed: 29513649]
30. Moreno-Jiménez EP et al. Adult hippocampal neurogenesis is abundant in neurologically healthy subjects and drops sharply in patients with Alzheimer's disease. Nat. Med 25, 554–560 (2019). [PubMed: 30911133]
31. Lebel C & Beaulieu C Longitudinal development of human brain wiring continues from childhood into adulthood. J. Neurosci 31, 10937–10947 (2011). [PubMed: 21795544]
32. Chang A, Nishiyama A, Peterson J, Prineas J & Trapp BD NG2-positive oligodendrocyte progenitor cells in adult human brain and multiple sclerosis lesions. J. Neurosci 20, 6404–6412 (2000). [PubMed: 10964946]

33. Gershon RC et al. NIH Toolbox for assessment of neurological and behavioral function. Neurology 80, S2–S6 (2013). [PubMed: 23479538]
34. Talley JL Children's Auditory Verbal Learning Test-2. Professional Manual (Psychological Assessment Resources, 1993).
35. Schmidt M Rey Auditory Verbal Learning Test: RAVLT: a handbook (Western Psychological Services, 1996).
36. CANTAB® (cognitive assessment software) http://www.cantab.com/ (Cambridge Cognition, 2018).
37. Grizzle JE The two-period change-over design and its use in clinical trials. Biometrics 21, 467–480 (1965). [PubMed: 14338679]
38. Fieremans E, Jensen JH & Helpern JA White matter characterization with diffusional kurtosis imaging. Neuroimage 58, 177–188 (2011). [PubMed: 21699989]
39. Jelescu IO et al. In vivo quantification of demyelination and recovery using compartment-specific diffusion MRI metrics validated by electron microscopy. Neuroimage 132, 104–114 (2016). [PubMed: 26876473]
40. Smith SM et al. Tract-based spatial statistics: voxelwise analysis of multi-subject diffusion data. Neuroimage 31, 1487–1505 (2006). [PubMed: 16624579]
41. Pereira AC et al. An in vivo correlate of exercise-induced neurogenesis in the adult dentate gyrus. Proc. Natl Acad. Sci. USA 104, 5638–5643 (2007). [PubMed: 17374720]
42. Kahalley LS et al. Superior intellectual outcomes after proton radiotherapy compared with photon radiotherapy for pediatric medulloblastoma. J. Clin. Oncol 38, 454–461 (2020). [PubMed: 31774710]
43. Moxon-Emre I et al. Impact of craniospinal dose, boost volume, and neurologic complications on intellectual outcome in patients with medulloblastoma. J. Clin. Oncol 32, 1760–1768 (2014). [PubMed: 24516024]
44. Wellek S & Blettner M On the proper use of the crossover design in clinical trials: part 18 of a series on evaluation of scientific publications. Dtsch. Arztebl. Int 109, 276–281 (2012). [PubMed: 22567063]
45. Zammit AR et al. Roles of hippocampal subfields in verbal and visual episodic memory. Behav. Brain Res 317, 157–162 (2017). [PubMed: 27646772]
46. Zheng F et al. The volume of hippocampal subfields in relation to decline of memory recall across the adult lifespan. Front. Aging Neurosci 10, 320 (2018). [PubMed: 30364081]
47. Leszczynski M How does hippocampus contribute to working memory processing?. Front. Hum. Neurosci 5, 168 (2011). [PubMed: 22194719]
48. Curtis E et al. A first-in-human, phase I study of neural stem cell transplantation for chronic spinal cord injury. Cell Stem Cell 22, 941–950 (2018). [PubMed: 29859175]
49. Gupta N et al. Neural stem cell engraftment and myelination in the human brain. Sci. Transl. Med 4, 155ra137 (2012).
50. Ou Z et al. Metformin treatment prevents amyloid plaque deposition and memory impairment in APP/PS1 mice. Brain Behav. Immun 69, 351–363 (2018). [PubMed: 29253574]
51. Gantois I et al. Metformin ameliorates core deficits in a mouse model of fragile X syndrome. Nat. Med 23, 674–677 (2017). [PubMed: 28504725]
52. Luchsinger JA et al. Metformin in amnestic mild cognitive impairment: results of a pilot randomized placebo controlled clinical trial. J. Alzheimers Dis 51, 501–514 (2016). [PubMed: 26890736]
53. Lin Y et al. Evaluation of metformin on cognitive improvement in patients with non-dementia vascular cognitive impairment and abnormal glucose metabolism. Front. Aging Neurosci 10, 227 (2018). [PubMed: 30100873]
54. Dy ABC et al. Metformin as targeted treatment in fragile X syndrome. Clin. Genet 93, 216–222 (2018). [PubMed: 28436599]
55. Gibson EM et al. Neuronal activity promotes oligodendrogenesis and adaptive myelination in the mammalian brain. Science 344, 1252304 (2014). [PubMed: 24727982]

56. Sato Y et al. Grafting neural stem and progenitor cells into the hippocampus of juvenile, irradiated mice normalizes behavior deficits. Front. Neurol 9, 715 (2018). [PubMed: 30254600]
57. Babona-Pilipos R, Popovic MR & Morshead CM A galvanotaxis assay for analysis of neural precursor cell migration kinetics in an externally applied direct current electric field. J. Vis. Exp 2012, 4193 (2012).
58. Coles-Takabe BL et al. Don't look: growing clonal versus nonclonal neural stem cell colonies. Stem Cells 26, 2938–2944 (2008). [PubMed: 18757294]
59. Nusrat L et al. Cyclosporin A-mediated activation of endogenous neural precursor cells promotes cognitive recovery in a mouse model of stroke. Front. Aging Neurosci 10, 93 (2018). [PubMed: 29740308]
60. Spiller HA & Quadrani DA Toxic effects from metformin exposure. Ann. Pharmacother 38, 776–780 (2004). [PubMed: 15031415]
61. Hsia Y et al. Unlicensed use of metformin in children and adolescents in the UK. Br. J. Clin. Pharmacol 73, 135–139 (2012). [PubMed: 21762204]
62. Vakil E, Greenstein Y & Blachstein H Normative data for composite scores for children and adults derived from the Rey Auditory Verbal Learning Test. Clin. Neuropsychol 24, 662–677 (2010). [PubMed: 20155574]
63. Riggs L et al. Exercise training for neural recovery in a restricted sample of pediatric brain tumor survivors: a controlled clinical trial with crossover of training versus no training. Neuro Oncol. 19, 440–450 (2017). [PubMed: 27555603]
64. Dale AM, Fischl B & Sereno MI Cortical surface-based analysis. I. Segmentation and surface reconstruction. Neuroimage 9, 179–194 (1999). [PubMed: 9931268]
65. Fischl B, Liu A & Dale AM Automated manifold surgery: constructing geometrically accurate and topologically correct models of the human cerebral cortex. IEEE Trans. Med. Imaging 20, 70–80 (2001). [PubMed: 11293693]
66. Ades-Aron B et al. Evaluation of the accuracy and precision of the diffusion parameter EStImation with Gibbs and NoisE removal pipeline. Neuroimage 183, 532–543 (2018). [PubMed: 30077743]
67. Veraart J et al. Denoising of diffusion MRI using random matrix theory. Neuroimage 142, 394–406 (2016). [PubMed: 27523449]
68. Veraart J, Fieremans E & Novikov DS Diffusion MRI noise mapping using random matrix theory. Magn. Reson. Med 76, 1582–1593 (2016). [PubMed: 26599599]
69. Kellner E, Dhital B, Kiselev VG & Reisert M Gibbs-ringing artifact removal based on local subvoxel-shifts. Magn. Reson. Med 76, 1574–1581 (2016). [PubMed: 26745823]
70. Andersson JLR & Sotiropoulos SN An integrated approach to correction for off-resonance effects and subject movement in diffusion MR imaging. Neuroimage 125, 1063–1078 (2016). [PubMed: 26481672]
71. Collier Q, Veraart J, Jeurissen B, den Dekker AJ & Sijbers J Iterative reweighted linear least squares for accurate, fast, and robust estimation of diffusion magnetic resonance parameters. Magn. Reson. Med 73, 2174–2184 (2015). [PubMed: 24986440]
72. Avants BB et al. The Insight Toolkit image registration framework. Front. Neuroinformatics 8, 44 (2014).
73. Engvig A et al. Memory training impacts short-term changes in aging white matter: a longitudinal diffusion tensor imaging study. Hum. Brain Mapp 33, 2390–2406 (2012). [PubMed: 21823209]
74. Jenkinson M & Smith S A global optimisation method for robust affine registration of brain images. Med. Image Anal 5, 143–156 (2001). [PubMed: 11516708]
75. Jenkinson M, Bannister P, Brady M & Smith S Improved optimization for the robust and accurate linear registration and motion correction of brain images. Neuroimage 17, 825–841 (2002). [PubMed: 12377157]
76. Shirzadi Z, Crane DE, Robertson AD & Maralani PJ Automated removal of spurious intermediate cerebral blood flow volumes improves image quality among older patients: a clinical arterial spin labeling investigation.J. Magn. Reson. Imaging 42, 1377–1385 (2015). [PubMed: 25873287]
77. van Osch MJ et al. Quantitative cerebral perfusion MRI and CO2 reactivity measurements in patients with symptomatic internal carotid artery occlusion. Neuroimage 17, 469–478 (2002). [PubMed: 12482099]

78. Hendrikse J et al. Internal carotid artery occlusion assessed at pulsed arterial spin-labeling perfusion MR imaging at multiple delay times. Radiology 233, 899–904 (2004). [PubMed: 15486211]

79. Faul F, Erdfelder E, Lang A-G & Buchner A G *Power 3: a flexible statistical power analysis program for the social, behavioral, and biomedical sciences. Behavior Res, Methods 39, 175–191 (2007).

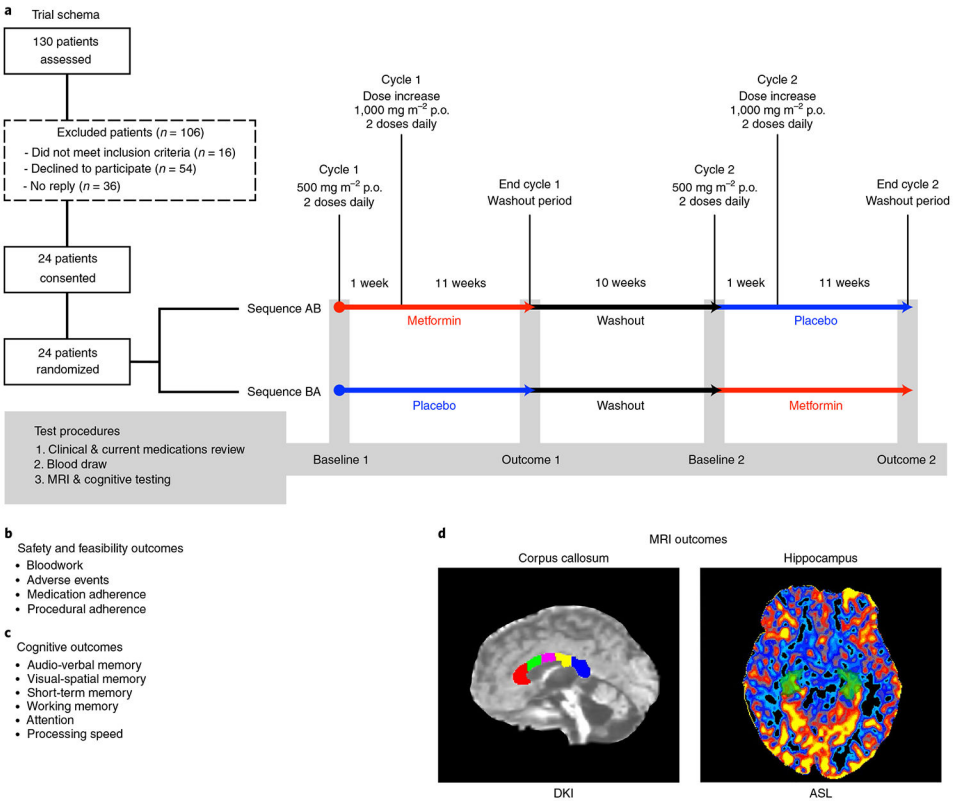

Fig. 1 | Pilot trial design and procedures.

a, Eligible participants were identified via database review and randomized to receive metformin or placebo in either an AB (metformin then placebo) or BA (placebo then metformin) sequence. MRI and cognitive testing were conducted at study entry (baseline 1), after ~12 weeks of treatment 1 (outcome 1), after a 10-week washout period at 22 weeks (baseline 2) and at the end of the trial at ~34 weeks (outcome 2). **b**, Safety and feasibility outcomes. **c**, Cognitive outcomes included tests of auditory-verbal memory using the CAVLT-2 or RAVLT[34,35] and tests of visual-spatial memory and working memory from the NIH Toolbox[33]. We also calculated a composite accuracy and latency score across tests of attention, short-term memory and processing speed from the CANTAB[36]. **d**, MRI outcomes included WMTI metrics sensitive to myelin (AWF and extra-axonal radial diffusivity ($D_{e,\perp}$)). An AWF map is shown from within the corpus callosum acquired from DKI and arterial spin labeling (ASL) within the hippocampus. Both the corpus callosum and hippocampus were delineated using an anatomic T1 sequence and a semiautomated segmentation pipeline using FreeSurfer. DKI and ASL scans were registered with the anatomic T1 sequence to obtain the respective metrics within the corpus callosum and hippocampus.

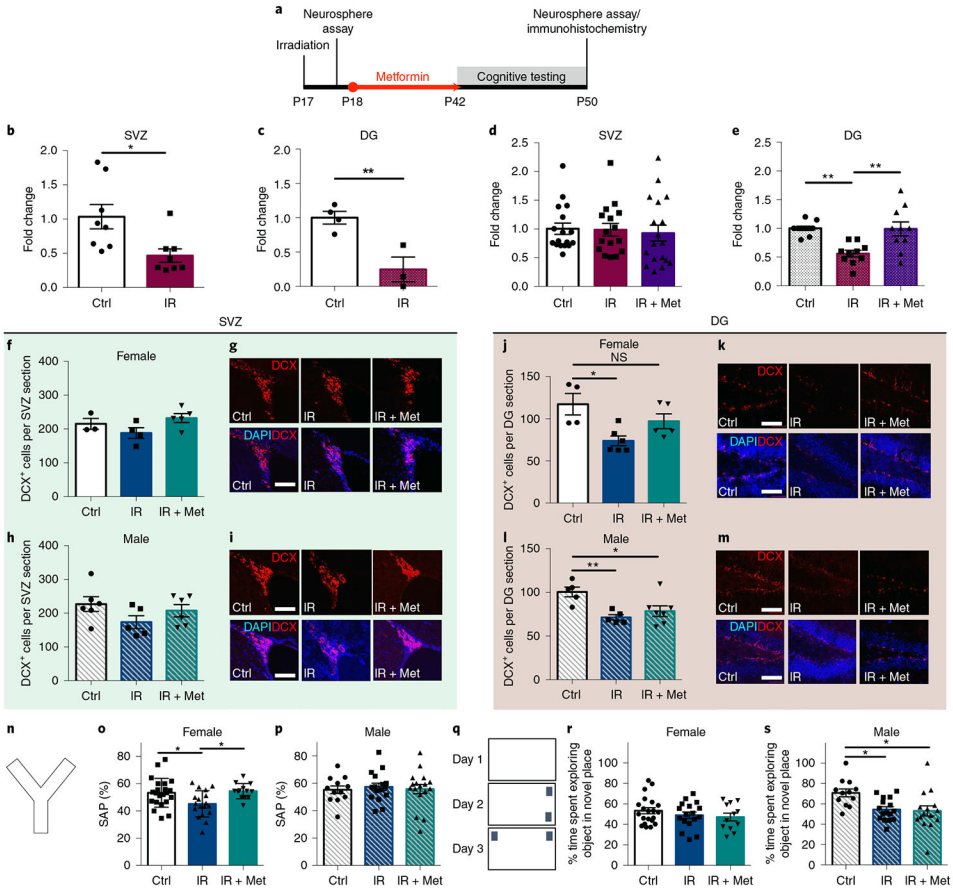

Fig. 2 | Cranial radiation leads to cellular and cognitive deficits and metformin is able to rescue these deficits in females.

a, Experimental schematic. **b**, Fold change in the number of neurospheres from the SVZ 2 d after radiation ($n = 8$ mice per group over three independent experiments; $t_{(14)} = 2.81$, $P = 0.01$; two-sided unpaired t test). Ctrl, control; IR, cranial radiation. **c**, Fold change in the number of neurospheres from the DG 1 d after radiation on P17 ($n = 4$ Ctrl and 3 IR mice over three independent experiments; $t_{(5)} = 4.04$, $P = 0.01$; two-sided unpaired t test). **d**,**e**, Fold change in the number of neurospheres from the SVZ ($n = 17$ Ctrl, 16 IR and 18 IR + Met mice over ten independent experiments; $F_{(2,48)} = 0.11$, $P = 0.89$; one-way ANOVA) (**d**) and DG ($n = 10$ mice per group over four independent experiments; $F_{(2,27)} = 9.81$, $P = 0.001$; Ctrl vs. IR, $P = 0.002$; IR vs. IR + Met, $P = 0.002$; one-way ANOVA with Tukey's test) (**e**) 5 weeks after radiation. Met, metformin. **f**,**h**, Numbers of DCX^+ cells per section in the female ($n = 3$ Ctrl, 4 IR and 5 IR + Met mice over three independent experiments; $F_{(2,9)} = 2.453$, $P = 0.14$; one-way ANOVA) (**f**) and male ($n = 6$ Ctrl, 5 IR and 6 IR + Met mice over three independent experiments; $F_{(2,14)} = 1.77$, $P = 0.21$; one-way ANOVA) (**h**) SVZ after radiation and metformin treatment. **g**,**i**, DCX^+ cells in the SVZ of female (**g**) and male (**i**) mice (scale bars, 50μm). **j**,**l**, Numbers of DCX+ cells per section in the female ($n = 4$ Ctrl, 6 IR and 5 IR + Met mice over four independent experiments; $F_{(2,12)} = 6.22$, $P = 0.01$; Ctrl vs. IR, $P = 0.01$; Ctrl vs. IR + Met, $P = 0.30$; one-way ANOVA with Tukey's test) (**j**) and male ($n = 5$ Ctrl, 5 IR and 7 IR + Met mice over four independent experiments; $F_{(2,14)} = 7.00$, $P = 0.008$; Ctrl vs. IR, $P = 0.008$; Ctrl vs. IR + Met, $P = 0.030$; one-way ANOVA with

Tukey's test) (**l**) DG after radiation and metformin treatment. **k**,**m**, DCX^+ cells in the DG of female (**k**) and male (**m**) mice (scale bars, 50μm). **n**, Y maze apparatus. **o**,**p**, Spontaneous alternation performance (SAP) measured using the Y maze at P43 in females (n = 21 Ctrl, 17 IR and 12 IR + Met mice over 12 independent experiments; $F_{(2,47)}$ = 6.04, P = 0.005; Ctrl vs. IR, P = 0.02; Ctrl vs. IR + Met, P = 0.71; one-way ANOVA with Tukey's test) (**o**) and males (n = 12 Ctrl, 16 IR and 16 IR + Met mice over 12 independent experiments; $F_{(2,41)}$ = 0.11, P = 0.89; one-way ANOVA) (**p**). **q**, Novel place recognition apparatus. **r**,**s**, Percentage of time spent exploring objects in the novel place recognition task from P44-P46 in females (n = 21 Ctrl, 17 IR and 12 IR + Met mice over 12 independent experiments; $F_{(2,47)}$ = 0.98, P = 0.38; one-way ANOVA) (**r**) and males (n = 12 Ctrl, 16 IR and 16 IR + Met mice over 12 independent experiments; $F_{(2,41)}$ = 5.16, P = 0.01; Ctrl vs. IR, P = 0.02; Ctrl vs. IR + Met, P = 0.02; one-way ANOVA with Tukey's test) (**s**). *P < 0.05, **P < 0.01; NS, not significant. Data are represented as means ±s.e.m.

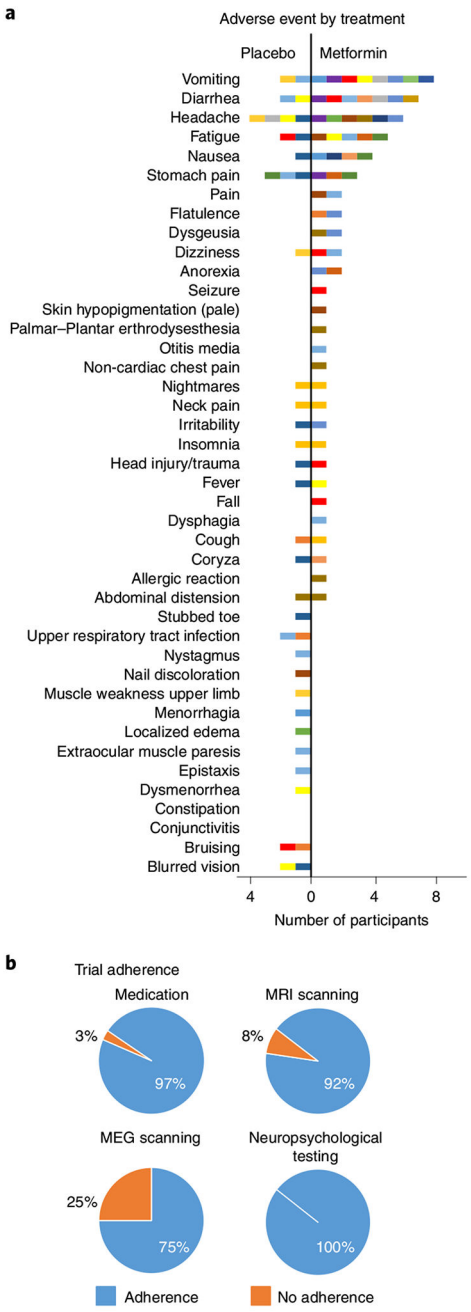

Fig. 3 | Pilot trial adverse events and adherence.

a, The frequency of all adverse events experienced during metformin and placebo treatment for all participants. For comparison purposes, the graph shows the frequency of adverse events recorded during metformin treatment. Each participant is represented by a single color, and participants who experienced multiple adverse events are represented with the same color in both the metformin and placebo panels. All adverse events are reported, including 15 adverse events that were not attributed to metformin by the attending physician (for example, seizure and head injury/trauma in a single participant). During treatment with metformin, 19 participants experienced at least one adverse event and 14 of these reported

multiple adverse events. One participant experienced nausea and diarrhea while being treated with metformin and withdrew from the study after 1 week. By comparison, when taking placebo, 13 participants experienced at least one adverse event (grade range 1-2) and 7 of these reported multiple adverse events. **b**, Adherence to taking the study pills and study procedures. Adherence was high except for magnetoencephalography (MEG) scanning, where there was a lack of usable neural data owing to poor adherence and motion artifact; this outcome was therefore not evaluated in the trial.

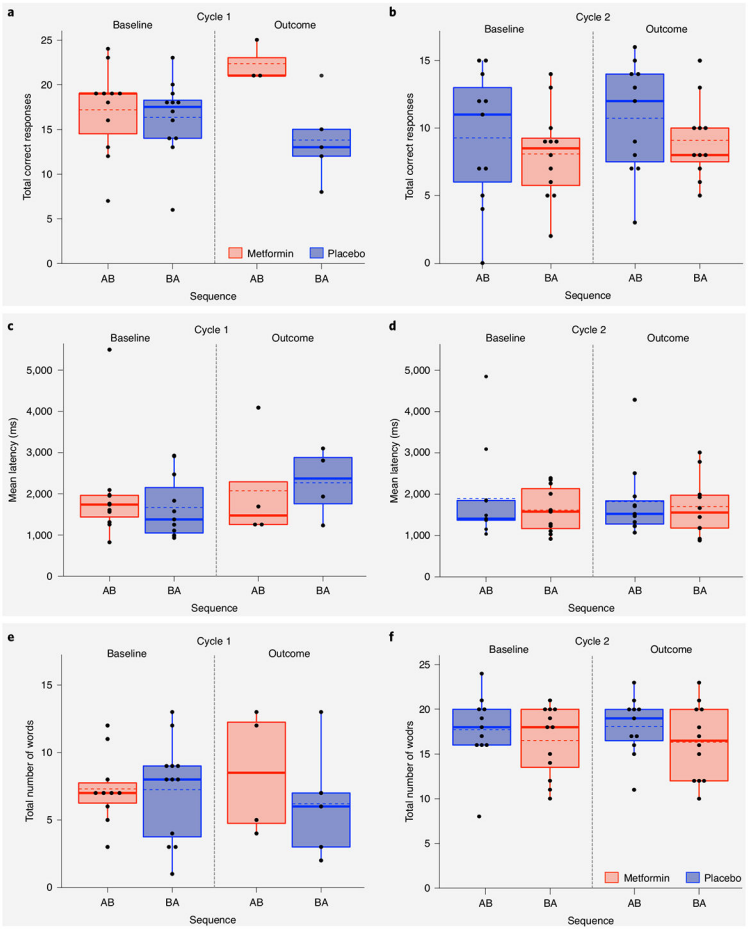

Fig. 4 |. Baseline and outcome data points for LSWM, average reaction time on the CANTAB tests and immediate recall on the CAVLT-2/RAVLT.

a–f, Box plots showing baseline and outcome assessment data points used for the following model: cognitive outcome = cycle + treatment + sequence + covariate (cognitive baseline) + (1∮ participant ID) + ε, where cycle, treatment and sequence are independent fixed effects and the cognitive measure is total correct responses on LSWM at cycle 1 (**a**) and cycle 2 (**b**); average reaction time across CANTAB tests at cycle 1 (**c**) and cycle 2 (**d**); and total number of words recalled for immediate recall at cycle 1 (**e**) and cycle 2 (**f**). True/unadjusted mean (dashed line) and median (solid line) values are shown for each sequence group. The metformin treatment condition is shown in red, and the placebo condition is shown in blue. The upper and lower limits of the boxes are the third and first quartiles (75th and 25th percentile), respectively. The whiskers extend to 1.5 times the interquartile range from the top (bottom) of the box to the furthest datum within that distance; data beyond this distance are represented individually as points.

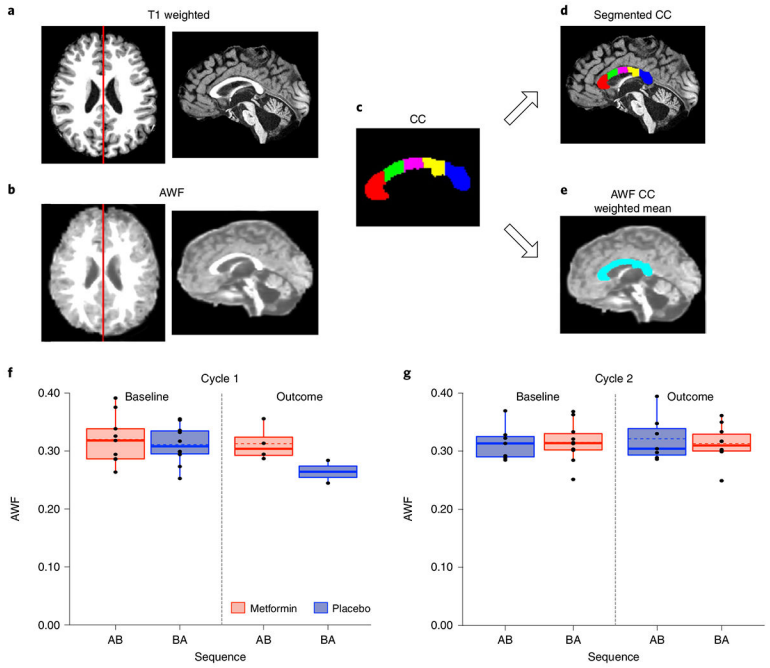

Fig. 5 |. Baseline and outcome data points for AWF within the corpus callosum.

a, T1-weighted image in the axial plane. The red line depicts the slice shown in the adjacent sagittal view. **b**, AWF image in the axial plane. The red line depicts the slice shown in the adjacent sagittal view. **c**, Segmentation of the corpus callosum (CC) from FreeSurfer (red, anterior CC; green, middle anterior CC; magenta, central CC; yellow, middle posterior CC; blue, posterior CC). **d**, Volumes calculated for each region of interest from the T1-weighted image were used to weight the mean AWF across the whole corpus callosum. **e**, A single weighted mean of the AWF across all corpus callosum regions was calculated. **f**,**g**, Box plots showing baseline and outcome assessment data points used for the following model: diffusion imaging outcome = cycle + treatment + sequence + covariate (diffusion imaging baseline) + (1| participant ID) + ε, where cycle, treatment and sequence are independent fixed effects and the diffusion imaging measure is AWF at cycle 1 (**f**) and cycle 2 (**g**). True/unadjusted mean (dashed line) and median (solid line) values are shown for each sequence group. The metformin treatment condition is shown in red, and the placebo condition is shown in blue. The upper and lower limits of the box are the third and first quartiles (75th and 25th percentile), respectively. The whiskers extend to 1.5 times the interquartile range from the top (bottom) of the box to the furthest datum within that distance; data beyond this distance are represented individually as points.

Table 1 |

Participant characteristics as a function of sequence

	Metformin then placebo	Placebo then metformin	*P* value
Sample size	11	12	
Sex (male)	7	6	0.41
Handedness (right)	10	10	0.54
Maternal education (years)	16.08	15.36	0.50
Paternal education (years)	15.58	14.46	0.48
Age at diagnosis (years)			0.57
Mean	7.26	6.44	
Standard deviation	3.34	3.63	
Range	(2-13)	(1-13)	
Age at first baseline assessment (years)			0.55
Mean	14.94	14.07	
Standard deviation	3.5	3.1	
Range	(8-20)	(10-20)	
Neurological exam immediately post-operatively			
Cerebellar signs (ataxia, dysmetria, dysdiadochkinesia)	10	4	0.01*
Hemiparesis	2	3	0.62
Cranial nerve deficit	6	1	0.03*
Visual disturbance (nystagmus, diplopia)	8	8	0.65
Mutism[a]	6	1	0.03*
Tumor type			0.57
Medulloblastoma	7	5	
Ependymoma	1	1	
Pineoblastoma	0	1	
Hemangioblastoma/sarcoma	0	1	
Sarcoma	0	1	
Germ cell	2	1	
Astroblastoma	0	1	
Astrocytoma	1	0	
Craniopharyngioma	0	1	
Tumor location			0.10
Supratentorial	2	5	
Subtentorial	9	7	
Extent of resection			0.93
Biopsy	2	3	
Subtotal	3	3	
Gross total	6	6	
Recurrence	3	0	0.06
Number of surgeries			0.47

	Metformin then placebo	Placebo then metformin	*P* value
One surgery	6	10	
Multiple surgeries	4	2	
Radiation dose and field			0.04*
Focal (5,400-5,940 cGy)/periventricular (2,100-3,000 cGy)	3	6	
Reduced dose cranial-spinal (2,340cGy) + tumor bed boost (3,240 cGy)	5	0	
Reduced/standard dose cranial-spinal (2,340-3,600 cGy)+ posterior fossa boost (1,800-3,240 cGy)	3	6	
Chemotherapy			0.21
None	1	3	
ACNS-0121 (carboplatin, cyclophosphamide, vincristine, etoposide)	1	0	
ACNS-0332 (carboplatin, cyclophosphamide, vincristine, cisplatin, G-CSF, isotretintoin)	0	1	
COG9961 (vincristine, iomustine, cisplatin)	1	0	
POG9631 (etoposide, cisplatin, cyclophosphamide, vincristine)	2	1	
COG99703 (thiotepa, carboplatin)	1	0	
ICE (carboplatin, ifosfamide, etoposide)	0	2	
SJMB96 and SJMB03 (vincristine, cisplatin, cyclophosphamide)	4	4	
Vindesine, bleomycin, high-dose methotrexate, cisplatin	1	0	
Carboplatin and etoposide	0	1	
Hydrocephalus at diagnosis			0.90
No hydrocephalus	4	3	
Hydrocephalus with no treatment	1	1	
Hydrocephalus requiring CSF diversion	7	8	

[a]Participants were classified as having mutism if they had diminished speech output, linguistic difficulties or dysarthria after surgery. Mutism is a transient dysfunction and had resolved in all participants by the time of baseline assessment. Significant differences at $P < 0.05$ are indicated with an asterisk. cGy, centigray; CSF, cerebrospinal fluid; G-CSF, granulocyte-colony stimulating factor.